SURFACE IMPEDANCE OF NORMAL AND SUPERCONDUCTORS AT 24,000 MEGACYLES PER SECOND

E. MAXWELL
P. M. MARCUS
J. C. SLATER

TECHNICAL REPORT NO. 109

MAY 2, 1949

RESEARCH LABORATORY OF ELECTRONICS
MASSACHUSETTS INSTITUTE OF TECHNOLOGY

The research reported in this document was made possible through support extended the Massachusetts Institute of Technology, Research Laboratory of Electronics, jointly by the Army Signal Corps, the Navy Department (Office of Naval Research) and the Air Force (Air Materiel Command), under Signal Corps Contract No. W36-039-sc-32037, Project No. 102B; Department of the Army Project No. 3-99-10-022.

MASSACHUSETTS INSTITUTE OF TECHNOLOGY

Research Laboratory of Electronics

Technical Report No. 109 May 2, 1949

SURFACE IMPEDANCE OF NORMAL AND SUPERCONDUCTORS AT 24,000 MEGACYCLES PER SECOND*

E. Maxwell**

P. M. Marcus***

J. C. Slater

ABSTRACT

The surface impedance of tin at 24,000 Mc/sec has been investigated in the range of temperatures from 2°K to 300°K, including both the superconducting and normal states, by means of a resonant-cavity technique. The experimental techniques are described and the data for the normal state discussed in terms of the theory of the anomalous skin effect given by Reuter and Sondheimer. Agreement is found between the general features of the theory and the data, although numerical estimates for the number of free electrons appear too low. An alternative derivation of the Reuter and Sondheimer integral equations is given. The superconducting data are analyzed in terms of a theory which combines the London and the Reuter and Sondheimer theories. The variation of penetration depth, λ, with temperature is found to be in agreement with other determinations. The best value for λ_o is estimated at 10^{-5} cm.

* This paper is based on a thesis submitted in partial fulfillment of the Degree of Doctor of Philosophy at M.I.T.

** Now with the Cryogenics Section, National Bureau of Standards.

***Now with the Office of Naval Research, London Branch.

SURFACE IMPEDANCE OF NORMAL AND SUPERCONDUCTORS AT 24,000 MEGACYCLES PER SECOND

I. INTRODUCTION

The work reported here represents part of a general program of investigation of the conductivity of metals at low temperatures and microwave frequencies, which was initiated in the Research Laboratory of Electronics at M.I.T. in November, 1945. Preliminary reports of some phases of this work have already been given elsewhere (1)(2)(3). The purpose of the present paper is to present a coordinated picture of some of the work which has been done and the results which have been accumulated to date.

There were originally two main points of interest. One of these was to obtain data on the behavior of superconductors in the microwave range to see if the superconducting properties persisted down to wavelengths of the order of a centimeter. An experiment of London (4) in 1940, at a frequency of 1500 Mc/sec had clearly indicated that the superconducting properties existed at that frequency. However, measurements at optical and infrared frequencies (5) had not shown any evidence of superconducting properties. It was felt that the range of wavelengths of the order of 1 to 10 centimeters might be a sort of "twilight" region for superconductivity and well worth investigation.

The program was initiated while the Collins Liquid Helium Cryostat (6) was under development at M.I.T., and the apparatus was designed around the peculiar requirements of the Collins Cryostat. The initial experiments were done at 3 cm, an especially convenient region from the microwave point of view. It was decided to work with lead in the first trials, largely because the experiments were to be performed in the first developmental cryostat whose operating characteristics were as yet unknown. It was felt that the initial probability of success would be greater with a material having a high transition temperature which could be reached without helium liquefaction. This factor was considered more important in the preliminary work than the convenience of working in the liquid-helium region.

Superconductivity in lead at 3 cm was successfully observed in early 1946. Later that year the bulk of the effort was shifted to 1.25 cm. Also, since lead was not an ideal material on which to work because of its inconveniently high transition temperature, attention was shifted from it to tin.

Although the initial interest was largely in the superconducting properties, it became clear by the early part of 1947 that there was a pronounced anomaly in the r-f conductivity at low temperatures. This had, of course, been noted by London (4) at 1500 Mc/sec but at 24,000 Mc/sec the effect was literally huge.

Coincidentally, work in this same field, at 1200 Mc/sec, was in progress at the Royal Society Mond Laboratory in Cambridge, and has already been reported by Pippard (7). Some measurements at 3 cm were also in progress by Fairbank at Yale, although his results have not yet appeared in published form.

Following Pippard's observations of the anomalous r-f conductivity, Reuter and Sondheimer developed their theory of this effect. A preliminary version of their paper was kindly made available to us in manuscript form in the fall of 1947, and it has now appeared in print (8). It was soon realized that their theory could be used to derive values for the number of free electrons per atom by comparison with experimental data, and could also be applied to the behavior of the normal electrons in superconductors in the London theory. Some preliminary results of these analyses have already been reported (2).

II. THE SURFACE IMPEDANCE OF A METAL

At high frequencies, the most useful way of characterizing the effect of a metal surface on an electromagnetic field is by means of the surface impedance. As pointed out by Pippard (7), this is particularly important at low temperatures where anomalous effects enter because the conductivity is no longer a precise concept. The current at a point in the metal is no longer proportional just to the field strength at that point, but is given by an integral over the entire field distribution in the metal, although still a linear expression in the field amplitude. Thus the usual exponential forms for the field in the metal, or more generally, wave-equation solutions which can be matched at the surface to the outside field, cannot be used to determine the effect of the metal on the radiation field, as in the usual skin-depth theory. Rather, we must use the surface impedance as giving the boundary condition at the metal surface. Because the field in the metal is so highly damped, this same simple boundary condition applies to a good approximation for arbitrary external fields. To illustrate the physical significance of the surface impedance, we shall give the attenuation and phase-velocity shift of a wave traveling between parallel metal plates in terms of the surface resistance R and reactance X of the metal, respectively. Finally, equations necessary to analyze the data give the Q and frequency shift of a resonant metal cavity in terms of R and X of the walls. The parallel-plate case is a special case of the cavity, but can be treated much more simply and used to define the useful concepts of a resistance and an inductive skin depth in terms of the surface impedance.

A. Definition of Surface Impedance

The extension of the concept of impedance to general radiation fields

is now well known (9), hence requires no detailed discussion. To define the surface impedance, consider a general radiation field at a metal surface. Assuming the field to be very strongly damped as we go into the metal (say in the z-direction), so that the z-derivative in the metal is much larger than the x- and y-derivatives, it can be shown that the field in the metal has essentially just tangential E and H components, E perpendicular to H.

The only important field components are, then, say E_x and H_y. The surface impedance may be defined as a ratio of tangential fields at the metal surface:

$$Z = R + iX = \frac{4\pi}{c}\left|\frac{E_x}{H_y}\right|_{z=0} = \frac{E_x}{\int_0^\infty J_x(z)dz} = \frac{4\pi ik}{c}\left[\frac{E_x}{\frac{\partial E_x}{\partial z}}\right]_{z=0} , \qquad (1)$$

where $k = \omega/c$. Since the x- and y-variations are slow compared to the z-variation, the former may be ignored in determining the field and Z from the intrinsic properties of the metal; one has merely to treat the normal incidence of a plane wave on an infinite plane conducting surface.

In free space, E_x and H_y in Gaussian units have the same magnitude; hence the wave impedance in the direction of propagation is

$$Z = \frac{4\pi}{c} \quad \text{Gaussian units} = 120\,\pi \text{ ohms} , \qquad (2)$$

(the conversion factor is 9×10^{11}; the ohm is the smaller unit).

For a metal with conductivity σ

$$\begin{aligned} E_x(z) &= E_x(0)\, e^{i(\omega t - Kz)} , \\ H_y(z) &= H_y(0)\, e^{i(\omega t - Kz)} , \\ K^2 &= -\frac{4\pi i\omega\sigma}{c^2} = \left(\frac{1-i}{\delta}\right)^2 , \quad \text{where } \delta = \left(\frac{c^2}{2\pi\omega\sigma}\right)^{1/2} ; \end{aligned} \qquad (3)$$

hence

$$Z = \frac{4\pi}{c}\cdot\frac{k}{K} = \frac{2\pi\omega\delta}{c^2}(1+i) = \sqrt{\frac{2\pi\omega}{c^2\sigma}}(1+i) . \qquad (4)$$

III. ATTENUATION AND PHASE-VELOCITY SHIFT FOR A WAVE BETWEEN PARALLEL METAL PLATES OF ARBITRARY Z

We illustrate by a direct simple calculation the relation of R to attenuation, and X to the phase velocity of a wave traveling in the Z direction between parallel metal surfaces (normal to the Y direction) as a simple special case of the calculation of Q and frequency shift of a resonant cavity in terms of R and X of the walls. The latter relations are needed to find R and X from the data. This is the analogue, in high-frequency language,

of Pippard's discussion of a parallel-plate transmission line by low-frequency methods (7) (i.e., capacitance and inductance per unit length). Analogous definitions of "inductive skin depth" and "resistive skin depth" can be given.

The field components of the traveling wave between the walls are E_y, E_z and H_x and are combinations of

$$e^{(-iK_z z \mp iK_y y + i\omega t)}$$

(where $K_y^2 + K_z^2 = k^2$), and are slightly perturbed from the plane wave which would exist with perfectly conducting walls. For simplicity, we assume no variation in the x-direction. H_x is then symmetric and E_z antisymmetric about an origin midway between the walls. The boundary condition at the walls is satisfied by matching impedances in the y-direction.

With

$$\begin{aligned} E_z &= E_{zo} \sin K_y y \; e^{(-iK_z z + i\omega t)} , \\ H_x &= \frac{ik}{K_y} E_{zo} \cos K_y y \; e^{(-iK_z z + i\omega t)} , \end{aligned} \tag{5}$$

$$\frac{4\pi}{c} \left[\frac{E_z}{H_x} \right]_{y=\frac{d}{2}} = \frac{4\pi}{cik} \tan \frac{K_y d}{2} = Z \quad . \tag{6}$$

Now $K_z \sim k$, hence $K_y \ll k$; further $kd \sim 1$ for the microwave region and $K_y d \ll 1$. It follows then that

$$K_y^2 = \frac{icZ}{2\pi} \frac{k}{d} \tag{7}$$

and

$$K_z = k\left(1 + \frac{c}{4\pi kd} (X - iR) + \ldots \right) \quad . \tag{8}$$

The wave attenuation is equal to

$$\mathrm{Im}(K_z) = \frac{Rc}{4\pi d} \quad . \tag{9}$$

Equation (9) also follows from the general formula for power flow into the walls, using the Poynting vector. The phase velocity is given by

$$\text{phase velocity} = \frac{\omega}{\mathrm{Re} K_z} = \frac{\omega}{k\left(1 + \frac{Xc}{4\pi kd}\right)} \simeq c\left(1 - \frac{Xc^2}{4\pi\omega d}\right) \quad . \tag{10a}$$

The inductive skin depth δ' has been defined (7) as the distance the walls should be set back (and considered perfectly conducting) in calculating the inductance between them, for the purpose of determining the wave velocity

from the inductance and capacitance per unit length. (The capacitance is calculated using the original spacing.) The treatment of the previous paragraph may be extended to obtain the idea of an inductive skin depth without resorting to the concepts of inductance and capacitance. Thus we may replace a layer of the metal, of thickness δ', by a layer of high-dielectric material having zero conductivity. The tangential magnetic field can penetrate this layer but not the normal electric field. We set up fields in δ' like those of Eq.(5), replacing k by $k\sqrt{\epsilon}$, match impedances at the surface $y = d/2$. We then find

$$K_y^2 = -\frac{2k^2\delta'}{d} \tag{10b}$$

analogous to (7), and

$$z = (1 + \frac{\delta'}{d}) \tag{10c}$$

analogous to (8). Comparing Eq.(10c) with Eq.(10a) we obtain

$$\delta' = \frac{Xc^2}{4\pi\omega} \quad . \tag{10d}$$

Another approach would be to define δ' such that the magnetic energy stored in a layer of thickness δ' (between the plates) is equal to the magnetic energy stored in the metal. It is easily verified that this definition also leads to Eq.(10d).

The resistive skin depth δ is the usual skin depth when the ordinary conductivity theory can be used, hence is given by Eq.(4), namely

$$\delta = \frac{c^2R}{2\pi\omega} \quad .$$

δ may also be defined as the depth of a layer in which the mean-square total current in the metal $J^2 = 1/2\left|cH_{tan}/4\pi\right|^2$ flows uniformly and which has a conductivity related to the given surface resistance R by the usual relation Eq.(4)

$$R = \sqrt{\frac{2\pi\omega}{c^2\sigma}}$$

such that the d-c losses in the layer ($J^2/\sigma\delta$ per cm^2 of wall) are the same as the high-frequency losses.

In practice, the surface impedance is not measured directly, but may be calculated from the directly observable parameters of the resonant cavity, namely the Q and the resonant frequency. The Q to which we refer is the unloaded Q, which is defined as

$$Q = \omega \frac{\text{Energy Stored in the Cavity}}{\text{Energy Dissipated in the Walls/Second}} \quad .$$

The Q is inversely proportional to the surface resistance of the cavity resonator. The resonant frequency, on the other hand, depends primarily on the geometry and only to a second order on the surface reactance. Such information as we can get on the surface reactance depends upon the observation of a second-order effect and is, therefore, more difficult to obtain.

The analysis of a given cavity to yield the characteristic modes and frequencies, and the effect of a perturbation of the ideal boundary conditions on the characteristic frequencies, is given by Slater (10) (pp. 473-475, especially III-59). Generalizing III-56 and III-59 for arbitrary surface impedance (and changing units) gives

$$\frac{1}{Q} - 2i\,\frac{\Delta\omega}{\omega_a} = \frac{c^2(R + iX)}{4\pi\omega_a} \int H_a^2 da \quad , \tag{11}$$

where

ω_a = the unperturbed resonant frequency,

H_a = the magnetic field of the mode with volume integral over the cavity normalized to unity,

$\Delta\omega$ is the frequency shift or perturbation due to the finite surface reactance and the integral is over the surface area of the cavity.

The integral $\int H_a^2 da$ is a constant for a given cavity geometry and a given mode. Knowing what this constant is, we may evaluate R from the Q, and in principle we could evaluate X from the dimensions of the cavity (which would give ω_a) and the measured value of ω (which is the perturbed frequency). In practice this is difficult because it involves knowing the cavity dimensions very accurately, including those of the coupling orifice. It is also difficult to evaluate changes in X with temperature (which would be sufficient, since at room temperatures R and X should be equal) and it is possible only below about 20°K, where the frequency shift due to thermal contraction is very small and does not mask the effect due to changing surface reactance. This means that the only information on surface reactance which can be readily obtained is the change which occurs in the superconducting state. The absolute value is not evaluated by direct measurement.

IV. EXPERIMENTAL DETAILS

The experiments were carried out in the Collins Helium Cryostat (6) and the characteristics of the cryostat strongly influenced the design and limitations of the experiments. The experimental chamber in the cryostat is a circular cylinder approximately four inches in diameter and four feet deep. The liquid helium accumulates at the bottom of the chamber and the

experimental apparatus must be designed to project into the liquid. In operation, the temperature in the experimental chamber starts at room temperature and falls continuously until the liquefaction point is reached. This made it possible to make measurements continuously over this temperature interval but, since no temperature-stabilization apparatus was available, these were made while the temperature was falling at the rate of one or two degrees K per minute, and there was a lag of the order of 2°K between the readings of the thermometer and the temperature of the cavity. In the liquid-helium range, temperatures between 1.8°K and 4.2°K could be easily obtained and stabilized by maintaining the vapor pressure at the desired value. Temperature measurements in this range were made with a helium-vapor-pressure thermometer using the 1937 Leiden scale. Temperatures between room temperature and liquid helium were measured by means of a constant-volume gas thermometer.

Some of the preliminary work was done on lead cavities.* Because of the fact that the transition temperature for lead is 7.2°K, it was not possible to obtain any accurate data on the transition curve itself, although the initial and final values of the surface resistance were measured. The later work was done on tin at liquid-helium temperatures which made it possible to get much more accurate detail on the transition.

A maximum of about 5 liters of liquid helium could be produced which, because of the relatively large heat leaks present, would last for about three hours. For this reason there was some emphasis on speed of measurement in the design of the experiments, so that the maximum amount of data could be obtained per run. It was customary to take data on two cavities simultaneously, each fed from its own waveguide, with duplicate sets of accessory equipment. Since the cavities had to rest on the bottom of the cryostat they were fed through waveguides approximately four feet long. This arrangement imposed a number of limitations on the accuracy of measurement; these will be mentioned later.

When the engines of the cryostat were in operation, a considerable amount of vibration was produced. This necessitated shock-mounting of various kinds and materially increased the difficulty of measurement.

The cavities used were rectangular cavities operating in the TE_{102} mode. These cavities were formed by cold-pressing two identical halves with a steel die. These halves were then fastened together and to the waveguide. The parting plane occurred along a section of no transverse current flow

---

* These measurements were made by Dr. J. B. Garrison and we are indebted to him for the use of his data. It is understood that a complete account of his work is in preparation and should appear in print shortly.

which eliminated contact difficulties. Coupling between the cavity and the waveguide was effected by a small symmetrical inductive iris which was pressed out in the original forming operation and cut down to provide the proper degree of coupling.

The two halves of the cavity were soldered together, and to the waveguide, by soft soldering around the outside joint, in such a way that the solder did not penetrate to the interior of the cavity. A certain amount of soldering flux inevitably did get in and although the interior was subsequently flushed out with hot water and degreased, some contaminating material may have remained.

The cavities were continuously evacuated to about 10^{-5}mm Hg during operation. This was done by pumping through the waveguide which was sealed off by means of a mica disc and rubber gasket. Reflections from the disc were eliminated either by introducing auxiliary tuning screws to cancel out the reflection or by inserting an inductive iris directly over the disc to tune out the reflection. This iris was either a piece of metal foil, or was painted on the mica with silver paint. The iris technique was found to be substantially reflectionless (VSWR $\sim$1.01-1.02) over a band of a few hundred megacycles.

A. Methods of Measurement

The surface resistance as a function of temperature was found from Q measurements, while the change in surface reactance in the superconducting state was found by measuring the shift of the resonant frequency of the cavity.

Both relative and absolute types of Q measurement were made. In the relative type of measurement, we determine only the ratio of Q_w (the window Q) to Q_o (the unloaded Q). In the absolute method we determine the absolute value of Q_o. The relative measurements could be made very rapidly, and were consequently extremely useful because of the peculiar experimental conditions. Measurements at temperatures between room temperature and liquid-helium temperature had, of necessity, to be rapid because the temperature was changing continuously at an average rate of 1-2 degrees/min. Between room temperature and 20°K, the resonant frequency of the cavity changed at the rate of approximately 0.6 Mc/sec/sec due to the thermal contraction. This precluded making any detailed measurements of the resonance curve of the cavity in this region. The technique used was to frequency-modulate the klystron oscillator and observe the variation with frequency of reflected power from the cavity by means of a magic T bridge, crystal rectifier, and cathode-ray oscilloscope. There are two ways of using the magic T bridge. In one scheme, we measure the reflection from the cavity by using a matched

load in the opposite arm of the bridge. This is called the unbalanced bridge. The second method is a null method in which the cavity reflection is compared with a known and variable impedance so as to produce a null.

The unbalanced bridge is shown in the schematics of Figures 1 and 2.

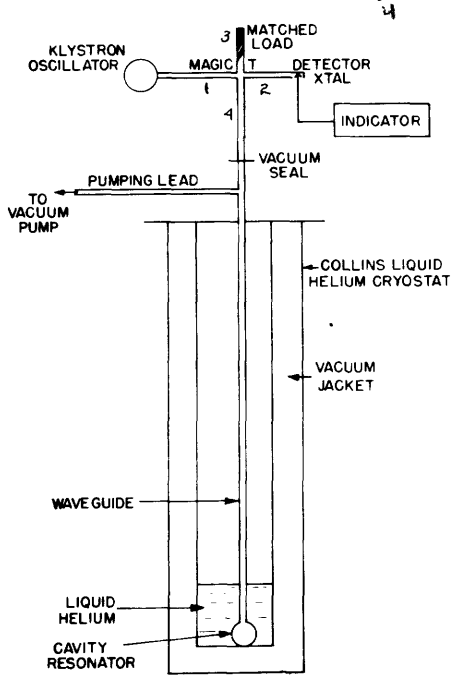

Fig. 1 Schematic diagram of the experiment.

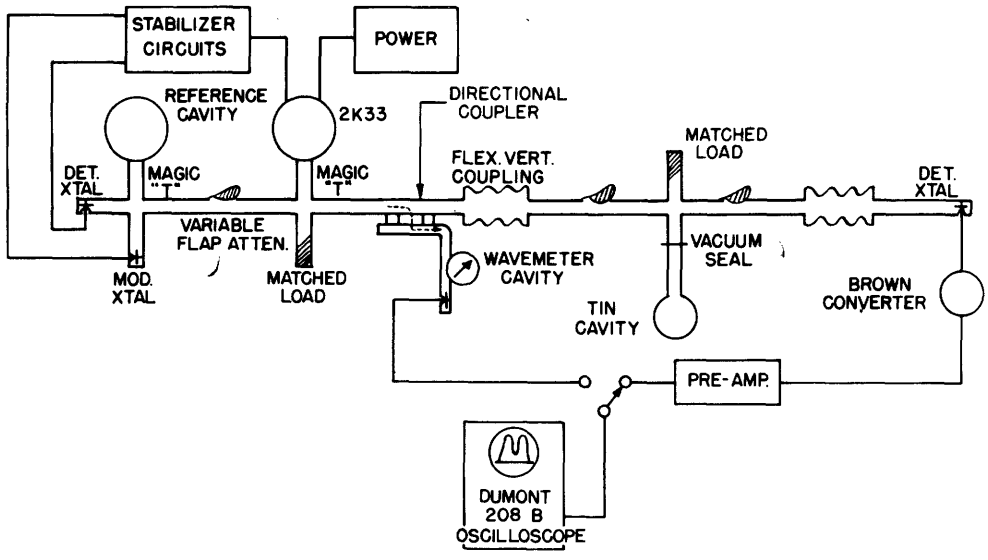

Fig. 2 Details of microwave plumbing for unbalanced bridge.

The type of pattern observed on the oscilloscope screen is shown in Figure 3. The klystron is frequency-modulated by impressing a 60-cycle sine voltage on the reflector, while a voltage from the same source, properly phased, is put on the horizontal deflecting plates of the oscilloscope. The dotted

curve is substantially the curve of power output vs. frequency for the klystron off resonance. This is modified by the cavity absorption, as shown by the solid line, when the klystron is swept past the resonant frequency of the cavity. The quantity observed is the ratio of h_1/h_2 which is the power-reflection coefficient of the cavity at resonance provided the crystal obeys a square law. In any case, if the crystal law is known, the VSWR on resonance may be easily calculated.

While h_2 is not observed directly, it can either be estimated if the resonance absorption dip is sharp enough, or it can be determined by detuning slightly to either side of resonance and observing the mode height. Under proper operating conditions, the height will not vary rapidly with frequency. An important consideration for proper operation is that the mismatch looking into the magic T from the cavity arm be kept quite low.

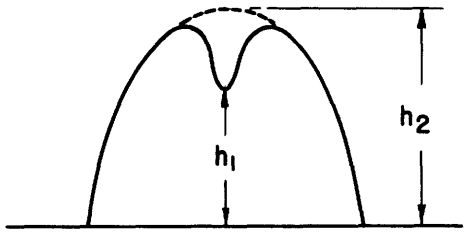

Fig. 3 Oscilloscope deflection pattern for unbalanced bridge. Vertical coordinate is amplitude; horizontal coordinate is frequency.

This is necessary for two reasons. First, the cavity and magic T are separated by some 80 wavelengths of line, which makes for rapid fluctuation with frequency of the power out of arm 2 (Figure 1) of the T. This means that h_2 as observed in Figure 3 will be a rapid function of frequency and therefore difficult to estimate accurately. The other consideration has to do with whether the cavity is overcoupled or undercoupled. Normally we would start with a cavity which is undercoupled at room temperature and consequently would have a small absorption dip in Figure 3. As the temperature falls, the cavity Q would increase, which would mean stronger coupling, and the depth of the dip would increase until the cavity became matched and the dip came down to the baseline. Finally, the cavity would become overcoupled and mismatched and the dip would start to decrease in depth. In the undercoupled cavity, the phase of the reflection is the same on resonance and far-off resonance, whereas in the overcoupled case there is a 180° phase difference for these two conditions. Consequently, a relatively small mismatch of the T may result in large errors if the cavity is overcoupled but is usually not important if the cavity is undercoupled. A mismatch of $1 + \Delta$ in VSWR may produce a fractional error of 2Δ in the voltage-reflection coefficient if the cavity is overcoupled. This means that if we wish to use overcoupled cavities, the magic T should be matched to about 1.01 or 1.02. As the temperature falls from room temperature to 20°K, the

resonant frequency of the cavity shifts by about 100 Mc/sec. With the magic T's used, it was not possible to maintain the VSWR down to 1.01 or 1.02 over the entire frequency interval and consequently the cavities were arranged so as to be undercoupled in this region. Once the frequency of the cavity ceases to increase (at about 20°K where the coefficient of linear expansion becomes vanishingly small), the cavity may be overcoupled, provided that the T has been matched up for this final frequency. However, at higher temperatures where the T will be mismatched, the long-line effect may be a nuisance in that it may distort the mode shape of Figure 3 and make it difficult to measure h_2.

The balanced bridge has the advantage of being independent of the T mismatch. This scheme is a null method and merely requires that the T be symmetrical. It is convenient to use the frequency-modulated klystron as the power source and to observe the crystal output on the oscilloscope. The impedance in the arm opposite the cavity is adjusted until a null is observed at resonance. The variable calibrated impedance takes the form of a matched variable attenuator backed by a sliding plunger fitted with a micrometer adjustment.

When using the balanced bridge arrangement, a correction must be made for the attenuation in the waveguide connecting the cavity and magic T. This is done by detuning the klystron off resonance and balancing the bridge, by adjusting the variable attenuator and plunger. This attenuator setting (in db) is then subtracted from the attenuator setting for balance on resonance. In the unbalanced bridge method, no explicit correction is made for guide attenuation since this enters equally in both h_1 and h_2.

One would like to be able to measure a given cavity in both the normal and superconducting states. In the normal state, the total change in Q for tin and lead at 24,000 Mc/sec is about 7 or 8 to 1 from 300°K to 4°K. For tin in the superconducting state, there is a further change of 10 to 1 between 3.7°K, and 2.2°K while for lead it is about 70 to 1 (between 7.2°K and 2°K).

Using the unbalanced bridge, one can measure a change of about 70 to 1 if the cavity is allowed to go from a strongly undercoupled to a strongly overcoupled condition. The precision of measurement is poor, however, in the region where the cavity is nearly matched. The optimum range of VSWR for this technique is between about 2 and 15. With the balanced-bridge technique, on the other hand, the optimum range is between 1 and 3 (overcoupled or undercoupled). The limitation in this case is set by the correction for the waveguide attenuation.

The measurements on tin were carried out with the unbalanced bridge exclusively. A cavity which was strongly undercoupled at room temperature

with a VSWR of about 10 had a VSWR of about 1.4 at 4°K. In going through the superconducting transition, the cavity went from an undercoupled to an overcoupled condition ending up with a VSWR of about 7. However, the steep part of the transition occurred just about where the cavity was matched and the precision poor. For accurately mapping out the transition region, it is better to use a cavity which does not go through a match. One with an initial VSWR of 10 gives good precision on the steep part of the curve. The data on tin were taken with one cavity of the first kind in both the normal and superconducting regions, and two of the second kind for measurements in the superconducting region only.

The measurements on lead were carried out using an unbalanced bridge for the measurements between 2°K and 20°K, and the balanced bridge between 20°K and 300°K. For the first-mentioned temperature interval, the cavities were strongly undercoupled to start with and ended up strongly overcoupled. No attempt was made to take any data on the steep part of the transition curve, due to the lack of adequate temperature control. The cavities used for measurements in the normal state started out undercoupled with a VSWR of about 3 and ended up just above the transition overcoupled with about the same mismatch.

The above-mentioned measurements gave the VSWR or Q_w/Q_o as a function of temperature. Q_w is constant with temperature, provided that the cavity undergoes no deformation in the temperature-cycling process. In order to determine the absolute value of Q_o at all temperatures, the absolute value was determined by taking complete resonance curves at one or two convenient fixed temperatures. In particular, room temperature and 4.2°K were the two fixed points used. This technique required that the oscillator be stabilized and that its frequency be variable in small increments. The scheme of Figure 4 was used to achieve these ends. A 2K-33 was stabilized to a resonant cavity and the working oscillator, which was a 2K-50, was tied to the 2K-33 by means of an i-f link which consisted of a commercial Hallicrafter VHF receiver. The operating frequency of the 2K-50 was conveniently varied by tuning the VHF receiver. The frequency stability of this arrangement was essentially that of the master oscillator. In these experiments, this was estimated as about 50 kc.

Measurements were made using the unbalanced magic T bridge at 4.2°K and a slotted section at room temperature. This gave two points which established the absolute values for the curve obtained from the relative measurements.

The arrangement of master and slave oscillators described above was used to measure the change in surface reactance as the cavity went superconducting. The quantity observed was the shift in resonant frequency relative to the resonant frequency at the transition temperature. This shift

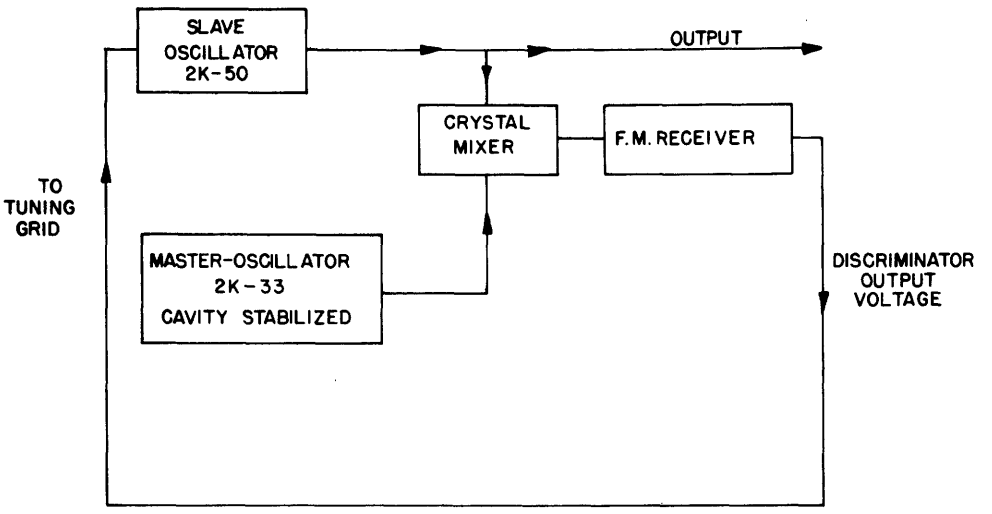

Fig. 4 Block diagram of master and slave oscillator arrangement.

was observed continuously as the temperature was lowered.

The nature of these experiments does not warrant any sophisticated analysis of precision indices but we may give the following estimates of the uncertainties in the measurements, based on some approximate considerations.* For the unbalanced-bridge method of measuring VSWR in the normal state, these range from 10 percent at a VSWR of 10 to about 6 percent at a VSWR of 1.5. For normalized VSWR in the superconducting state (ratio of VSWR to VSWR just above the transition temperature), these are of the order of 9 percent at 3.7°K and 20 percent at 2.1°K.

V. THE NORMAL STATE

The results of the measurements on tin and lead** are given in Figure 5. These figures compare the measured value of the surface resistance at 24,000 Mc/sec with the value calculated from the classical formula using the measured value of the d-c resistivity. It is seen that even at room temperatures there is a divergence of 10 or 15 percent between the measured and the calculated values. This sort of behavior has been observed before and is presumably due to a condition of surface roughness. Down to about 30°K the two curves continue parallel, but below 30°K anomalous behavior sets in rapidly. This phenomenon is, of course, the mean-free-path effect.

The first suggestion that consideration of electron mean free paths would modify the surface resistance properly was made by H. London (4).

---

* Cf. E. Maxwell, Ph.D thesis, M.I.T., 1948 (Appendix). Cf. J. B. Garrison, Ph.D thesis, M.I.T., 1947.

** Pb from M.I.T. Ph.D. thesis, J. B. Garrison, 1947.

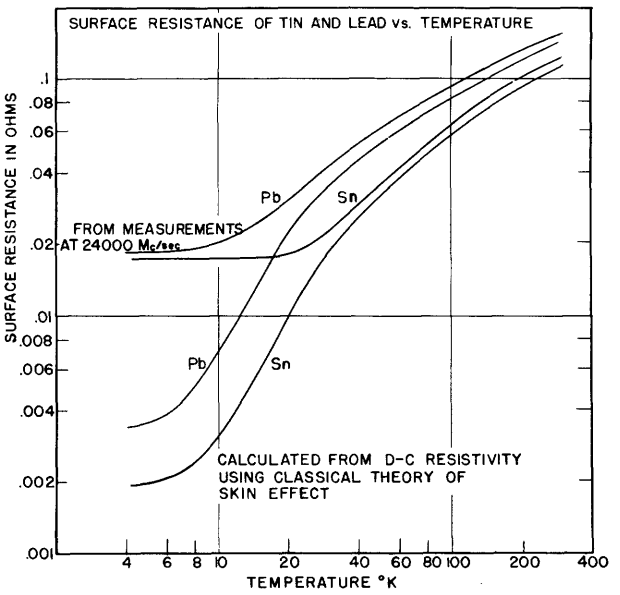

Fig. 5 Surface resistance of Sn and Pb in the normal state. Pb data by J. B. Garrison.

A. B. Pippard (7) made use of this idea in an approximate way which revealed most of the general physical behavior. Finally G. E. H. Reuter and E. H. Sondheimer (8) derived the integro-differential equation for the field which follows precisely for this model and solved two limiting cases rigorously. This work made use of the Boltzmann equation for the electron-distribution function which was solved using boundary conditions at the metal surface and infinity (to first-order terms in the field), and applied it to calculate the current in terms of the field. Pippard mentions a kinetic derivation of an integral equation which differs slightly from that of Reuter and Sondheimer and also is not in simplest form for solution by Fourier Integral methods. He makes little use of it except in a qualitative way, but bases his calculations on his "effectiveness concept". In this country, B. Serin (11) attempted to use a distribution-function, Boltzmann-equation approach to describe the electron behavior, and R. J. Harrison (12), at M.I.T. independently developed a kinetic approach. Both of these men attempted to find equivalent conductivities, rather than to solve an integral equation for the field, and they did not make use of the very fruitful description in terms of the surface impedance. Serin's results on the distribution function were shown to be incorrect (11) since they do not satisfy the boundary conditions at the metal surface. When the English work appeared, it became evident that the kinetic approach of Harrison or Pippard could be used to derive the integral equation.

The kinetic approach is given in Appendix I as a useful alternative to the distribution-function approach because it gives a clearer physical picture of the origin of the various contributions to the current at a point in the metal. This derivation now has more significance than when

Pippard indicated the problem could be approached this way (without giving details) since the integral equation has been solved. We shall obtain the integral equation in precisely the form of Reuter and Sondheimer and point out why Pippard's form is different.

The calculations made here are based on the familiar simple model of the electrons in a metal as forming a degenerate Fermi gas. Equilibrium is maintained by collisions with the lattice of positive ions (actually, lattice vibrations and irregularities). The energy of an electron is proportional to the velocity squared, but the mass is not necessarily the free-electron mass. In the presence of an electric field, electrons acquire small drift velocities in the direction of the field between collisions. The average drift velocity at a point determines the electric current there. Two basic constants will determine electron behavior, n the number of free electrons per cm^3, and ℓ the mean-free path for electrons at the edge of the Fermi distribution; $\ell = \tau v_M$ where v_M is the maximum velocity of the Fermi distribution, τ is the mean time between collisions, and the relaxation time of the electron distribution.

We shall derive the expression which follows from the free-electron model for the current in a metal in terms of the electric field, and combine it with Maxwell's equations to yield an integro-differential equation for the field. The solution of this equation yields the field in the metal, and the derivative at the surface yields the surface impedance of the metal. In the low-temperature region, the surface resistance at high frequencies will deviate from the predictions of ordinary skin-depth theory in the observed manner.

In the theory of Reuter and Sondheimer and in the equivalent treatment of Appendix I, the expression for the surface impedance is given finally in the form

$$Z = -\frac{4\pi i\omega\ell}{c^2}\frac{f(0)}{f'(0)} \quad , \tag{12a}$$

where f(x) gives the field distribution in the metal and f'(x) its derivative. Only the values of these functions at the surface are involved. In addition to n, ℓ, v_M and τ, it is useful to introduce the following parameters:

$$\sigma = \frac{\epsilon^2}{h}\frac{2\pi^{1/3}}{3^{1/3}}n^{2/3}\ell \quad , \tag{13}$$

$$\alpha = \frac{2\pi^{4/3}3^{2/3}}{hc^2}\epsilon^2\omega n^{2/3}\ell \quad , \tag{14}$$

$$A = \frac{3^{5/18}\, 2^{1/6}\, \pi^{5/4}\, h^{1/3}\, \omega^{2/3}\, n^{-2/9}}{c^{4/3}\, \epsilon^{2/3}}$$

$$= \frac{4\pi\omega}{c^2}\sqrt{\frac{3}{8}}\,\frac{\ell}{a^{1/3}} = \sqrt{\frac{2\pi\omega}{c^2}}\,\frac{a^{1/6}}{\sigma^{1/2}} \quad , \tag{15}$$

$$\delta = \frac{c}{\sqrt{2\pi\omega\sigma}} = \frac{3^{1/6}}{2\pi^{2/3}}\,\frac{h^{1/2}c}{\epsilon\omega^{1/2}}\,\frac{1}{n^{1/3}\ell^{1/2}} \quad , \tag{16}$$

where σ and δ are the ordinary d-c conductivity and classical skin depth, respectively, ϵ is the electronic charge, h and c have their customary meanings.

In terms of these other parameters, Z may be written as

$$Z = i\sqrt{\frac{8}{3}}\, A a^{1/3}\, \frac{f(0)}{f'(0)} \quad . \tag{12b}$$

Reuter and Sondheimer show the form of this function in Figure 1 of their paper (8). In Figure 6(b) we have re-plotted the function R/A to logarithmic coordinates. The two cases p = 0 and p = 1 correspond, respectively,

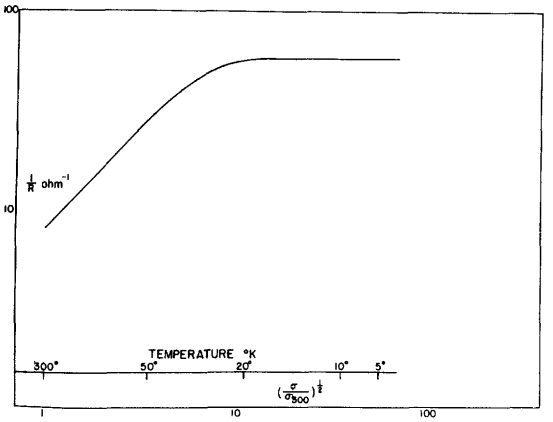

Fig. 6(a) Surface resistance data for Sn plotted in form for comparison with theory.

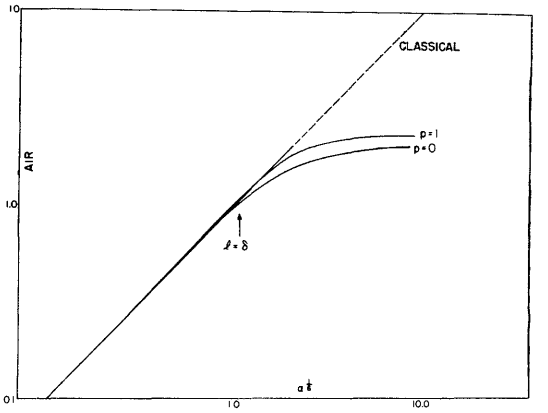

Fig. 6(b) Surface resistance as function of parameter α following Reuter and Sondheimer theory.

to diffuse and specular reflection at the surface of the conductor (see Appendix I for details). For very low temperatures, Z takes the limiting forms

$$Z \cong 0.4291A(1 + \sqrt{3}\, i) \quad , \quad p = 0 \quad ; \tag{17a}$$

$$Z = 0.4827A(1 + \sqrt{3}\, i) \quad , \quad p = 1 \quad . \tag{17b}$$

At room temperatures, Z is given by the classical formula

$$Z = \frac{2\pi\omega\delta}{c^2}(1 + i) = A\alpha^{-1/6}(1 + i) \qquad (18)$$

good for both p = 0 and p = 1.

One expects ℓ to depend on the temperature T, increasing as T decreases until the region of residual resistance is reached, but n should be independent of T. At a given frequency, A depends only on n, hence should not depend on T.

The data consist of $\sigma(T)$, R(T) (surface resistance, ReZ) at known frequency. Equation (13) then gives a relation between n and ℓ; Eq.(17a) or Eq.(17b) gives A from the limiting low-temperature value of R, hence a value of n from Eq.(13). Thus n and $\ell(T)$ may be deduced without using a value for the electron mass m, or, equivalently, the maximum Fermi velocity v_M. The latter is required to deduce the relaxation time τ.

The theory predicts the dependence of R/A on α. Hence, plotting 1/R vs. $\sqrt{\sigma}$ on a log-log scale gives an experimental curve of the same shape but displaced from the universal curve of A/R vs. $\alpha^{1/6}$ (which is proportional to $\sigma^{1/2}$). Thus an overall check of the theory can be obtained. The best position of fit of the two curves gives an average value of n from the displacement of the scales. (Relation (18), $R = \sqrt{2\pi\omega/c^2\sigma}$ must hold between R and $\sqrt{\sigma}$ at high temperatures.)

It is possible that the theory is accurate at high temperatures (classical region) and at very low temperatures in the residual-resistance region, in both of which the idea of a mean-free path is valid, but is not accurate at intermediate temperatures. Only these regions can be expected to match then, and we can determine n essentially only from the limiting value of R, as mentioned above.

In Figure 6(a), the data for tin have been plotted in the form of 1/R vs. $(\sigma/\sigma_{300})^{1/2}$ in logarithmic coordinates. These are to be compared with Figure 6(b), the theoretical curves of Reuter and Sondheimer. The experimental and theoretical curves are of generally similar shape but, of course, any theory which predicts that the surface resistance at low temperatures becomes independent of the d-c resistivity, will give a curve of the same shape.

As mentioned above, by matching the experimental to the theoretical curves we should be able to derive a value for n, the number of free electrons. In practice, this amounts to simultaneously superposing the asymptotic and the initial linear portions of the curves, inasmuch as the curves do not match very well in the bends (probably due to the reasons quoted above). This procedure demands that the measured surface resistivity and d-c conductivity be consistent at room temperature or, in other words, that the curves of Figure 6(a) and 6(b) coincide at room temperature. The

procedure adopted here has been to decrease the measured surface-resistance data so as to bring them into agreement, at room temperature, with the figure computed from the d-c conductivity. This seems more reasonable than the opposite procedure, since the microscopic parameters of the metal which we seek to determine by this process are related to the true d-c conductivity and not to geometrical form of the surface.

The results of this analysis of our data, and of Pippard's (7), are given in the following table.

Number of Free Electrons per Atom
Calculated from Surface Resistance

Metal	Authority	Frequency Mc/sec	n (per atom) p = 0	p = 1
Sn	Pippard	1200	1.1	0.67
Sn	Our data	24000	0.20	0.12
Pb	Our data	24000	0.19	0.12
Hg	Pippard	1200	0.57	
Al	Pippard	1200	0.70	0.41
Cu	Pippard	1200	0.11	0.07
Ag	Pippard	1200	0.066	0.038
Au	Pippard	1200	0.021	0.011

Two facts are at once apparent. First, our data for Sn gives results which are considerably lower than Pippard's. Second, most of the values given are low. One would expect n to be of the order of one. With the exception of the figures derived from Pippard's data for Sn, Hg, and Al, the numbers are considerably smaller than 1. The numbers for Au, Ag, and Cu are especially low. For these metals, Mott and Jones (16) give an estimate of about 0.8 free electrons per atom.

It should be noted also that the number obtained by the fitting process is sensitive to very small changes in the fitting (apart from the uncertainty in p), due to the fact that the constants evaluated in the matching process have to be raised to the 9/2 power in the calculation process. These uncertainties, however, hardly seem adequate to account for the discrepancies noted; even after taking this into account, the numbers seem low.

A possible explanation for the low values of n may be that at low temperatures the surface roughness is more important than at high temperatures.* At low temperatures the mean free path (in bulk metal) may be

* Some recent results of W. B. Nowak of this Laboratory indicate that it is possible to obtain different values of n by altering the surface roughness.

considerably larger than the surface irregularities. Hence the latter may reduce the effective mean free path. This effect would reduce the values of n obtained.

Another aspect of this discrepancy hinges on the value of the d-c resistivity. The resistivity of our tin as determined by measurements on extruded wires, was 13.7×10^{-6} ohm cm as compared with the figure of 11.5×10^{-6} ohm cm given by Onnes and Tuyn for pure tin in the International Critical Tables. The reason for our high resistivity is not known, but it was checked on a number of different annealed samples. Pippard apparently did not measure the absolute resistivity of his samples, but assumed the values given in the tables. Furthermore, he used these values to establish the proportionality between Q and the surface resistance of his resonators. However, even making full allowance for this difference in the d-c resistivities, this could, at most, account for a factor of about 2, whereas the actual discrepancy is about 5.

It is interesting, further, to compare the asymptotic values of the surface resistance reached at low temperatures in our experiments with those found by Pippard. The surface resistance of Sn was 0.0175 ohms at 23910 Mc/sec as against 0.00147 at 1190 Mc/sec in Pippard's case. According to the Reuter and Sondheimer theory, this quantity should go as $\omega^{2/3}$, and consequently the surface resistance should be 7.4 times as great at the higher frequency. The actual ratio is 11.9. Part of this discrepancy may be due to the difference in the d-c resistivities at room temperature discussed in the previous paragraph. To eliminate this factor, we can multiply our figure of 11.9 by $(11.5/13.7)^{1/2}$, which has the effect of making our room-temperature surface resistance consistent with those of Pippard and brings the ratio down to 10. The discrepancy is still large.

The corrections for relaxation effects, according to the Reuter and Sondheimer theory, are quite small, as previously noted. For the case of tine, the theoretical value of the asymptotic surface resistance should be decreased by about 5 percent in our case, which is, incidentally, in the wrong direction to rectify the discrepancies noted in the values found for n, and in the frequency dependence of the low-temperature surface resistance.

VI. SURFACE RESISTANCE

A. Superconducting State

The variation of surface resistance with temperature for the tin cavities is shown in Figure 7. This figure includes three separate runs on Cavity L as well as points from successful runs on Cavities M and H. A set of smoothed values of R/Rt is given in Table IV. The transition temperature,

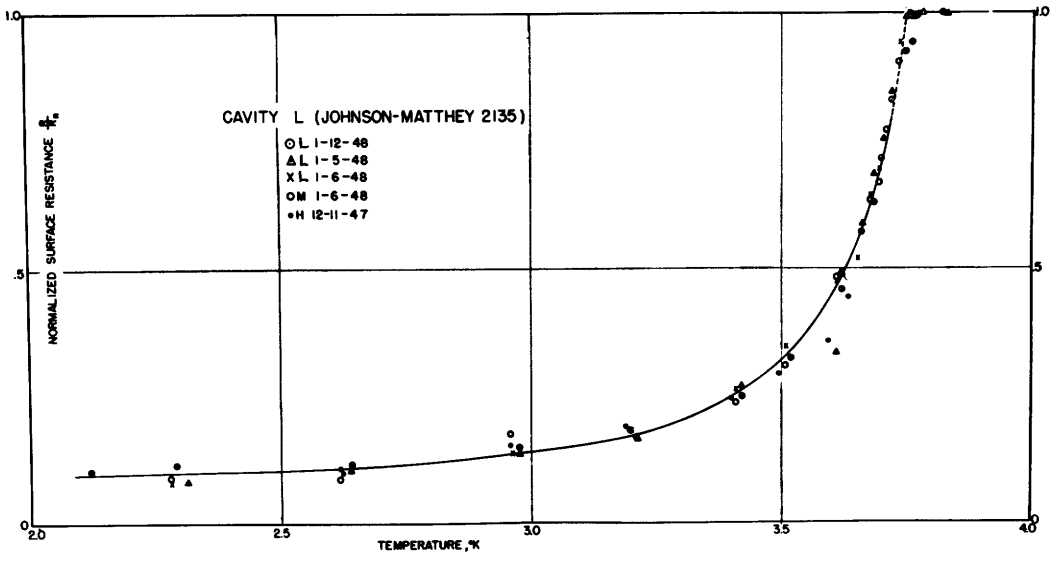

Fig. 7 Surface resistance of Sn in the superconducting state.

as nearly as can be judged, is 3.751°K. This is somewhat higher than that reported by others and may be due to residual strains.

The surface resistance is still appreciable at 2.1°K, the lowest temperature reached, and apparently is not headed for 0 at 0°K, but approaches a value of about 0.09. This same sort of behavior was noted by Pippard (7) at 1200 Mc/sec. The numerical value of R/R_t at 2.1°K reported by him was 0.009. Later work of Pippard's at 9200 Mc/sec, does seem to indicate, however, that the surface resistance may approach 0 at 0°K, so these discrepancies are still to be resolved.

The residual surface resistance may result from two separate mechanisms. First, the presence of impurities in the cavity may increase the apparent loss over the true value. Secondly, there is a possibility that a new type of absorption effect enters at these high frequencies, such that the electromagnetic quanta are large enough to induce some electronic transitions from the superconducting to the normal state. This would substitute normal for superconducting electrons and thus introduce losses by absorbing energy for the transition and by creating additional normal electrons which could lose energy to the lattice by collisions. This "photoelectric" absorption would, of course, be more effective at higher frequencies.

Either or both of these mechanisms may be operative in these experiments. In Pippard's 1200-Mc/sec experiments, he used dielectric spacers to support his resonator wires, and although he made corrections for the dielectric loss, it is conceivable that it was not entirely accounted for. The report of his work at 9200 Mc/sec contains no reference to such

corrections, so we do not know if they played any part in those experiments. In our experiments, no foreign bodies were deliberately inserted in the cavity, but it is possible that some contamination of the metal may have occurred in the process of fabrication.

Such absorption effects, whether by the pure metal itself or by normal inclusions within the cavity, are not included in the theories presented earlier in this chapter; and for the purpose of reducing the data by the techniques described, these effects should be subtracted. If the absorption effects are due to foreign bodies, the corrections are simple to make and can be done by merely subtracting the value of R/R_t approached at 0°K, together with an appropriate change of scale. If the absorption is caused by electronic transitions, then it is not clear how to make this correction, since the number of transitions per second may depend on the temperature. Since no other way of making the correction appears to be clearly indicated, we have subtracted the constant amount of 0.09 from R/R_t for the purpose of making our calculations.

Further experiments are evidently necessary to decide whether or not the finite residual resistance is really due to the edge of an absorption band. These experiments should be extended to include measurements at higher frequencies, lower temperatures, and to other materials, and should include control of the specimen purity. It is of some interest to compare the behavior of these tin cavities with some earlier results* obtained with Hillger lead cavities in this Laboratory, also at a frequency of 24,000 Mc/sec. In those experiments, it was not possible to observe the transition region with accuracy, due to the fact that the transition occurs at 7.2°K, just above the liquid-helium range. Between 4.2° and 2.0°K, however, measurements were possible, and, of course, the surface resistance could be determined fairly well just above the transition temperature. These measurements indicate a total change in surface resistance for lead of about 70 to 1 between 7.2°K and 2°K, about seven times as great as was observed with tin. This conforms to the expectation that the metal with the lower transition temperature should have an absorption band extending to lower frequencies.

B. Shift in Resonant Frequency of Cavity

The shift of resonant frequency of the cavity as a function of temperature is plotted in Figure 8 for two different cavities. The reason for the differences in the two curves is not known. For purposes of calculation the two curves were averaged.

---

* Due to J. B. Garrison.

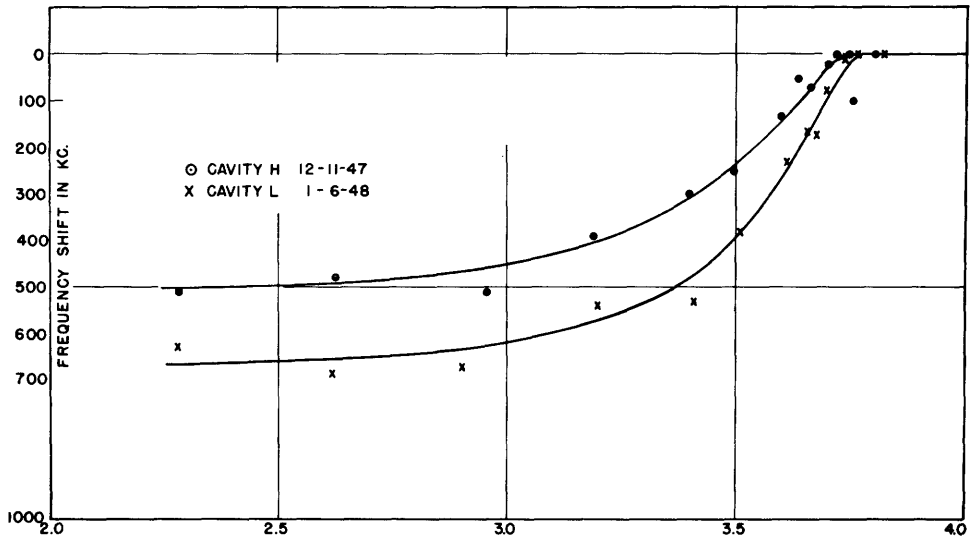

Fig. 8 Shift in resonant frequency of Sn cavity as a function of temperature.

C. Interpretation

The usual way of treating a superconductor in which normal as well as superconducting electrons are present is to consider the total current as consisting of two components which are separately identified with the two kinds of electrons. The superconducting electron current density is related to the electric field strength by the London theory and the normal electron density by either Ohm's law or whatever modification is deemed appropriate. Thus H. London (4) assumed the validity of Ohm's law in his treatment but used an effective value for the a-c conductivity much lower than the d-c conductivity; Pippard (7) used the "ineffectiveness concept". In our treatment, however, we use the theory of Reuter and Sondheimer to give the relation between the normal current density and the electric field. The Reuter and Sondheimer treatment is then modified by the addition of a term for the super current and the integral equations may be solved by the same general techniques. The surface resistance and reactance of the superconductor may then be expressed in terms of three parameters, δ_{et}, the resistive skin depth just above the transition, $\lambda(T)$, the static field penetration depth, and the fraction of normal electrons at any temperature, $f_N(T)$. If we assume a relation between $f_N(T)$ and $\lambda(T)$, such, for example, that the sum of normal and superconducting electrons is constant, then we can determine both. They may both be related to $\lambda_o = \lambda(0)$. By combining the information given by both the surface resistance measurements and the shift in resonant frequency of the cavity (which is related to the surface reactance) λ_o is evaluated.

The details of this treatment are given in Appendix II. We have also derived the formulas given by London and Pippard in terms of the same three parameters in order to exhibit the differences among these three modes of handling the problem.

D. Initial Slopes

According to the theory given in Appendix II the initial slope of the R/R_t curve should go as $\omega^{-2/3}$. Figure 9 is a logarithmic plot of the initial slope $d/dT\ (R/R_t)$ vs. the frequency, on which we have plotted Pippard's results at 1200 and 9200 Mc/sec and ours at 23910 Mc/sec, and fitted the best straight line. It is seen that the observed frequency variation is more nearly $\omega^{-0.48}$ or $\omega^{-1/2}$ rather than $\omega^{-2/3}$.

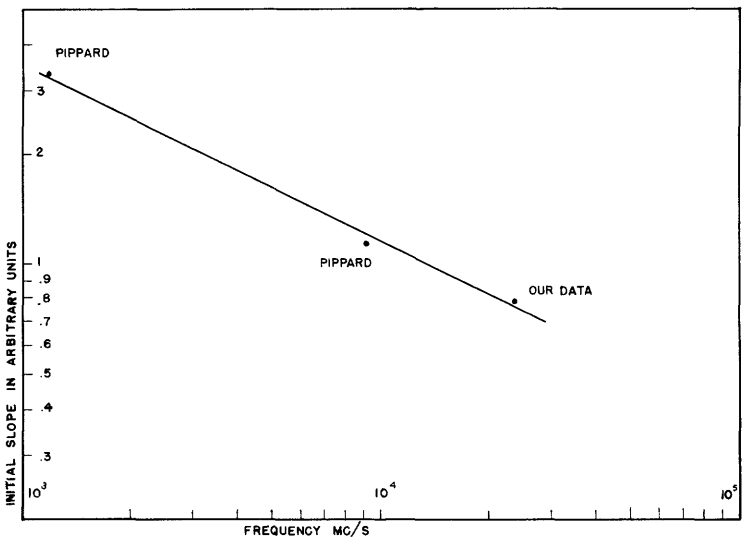

Fig. 9 Data on initial slopes of transition curves as a function of frequency.

Equation (77) of the Appendix II for the initial slope of the inductive skin depth indicates an initial negative slope. Further, since the inductive skin depth approaches λ_o as the temperature goes toward zero, the curve must have a maximum in the neighborhood of $T = T_t$. However, the data are not good enough to detect any detailed structure in this region.

E. Penetration Depths

In Figure 10 we have plotted curves of λ vs. T for our data on tin, calculated according to the data reduction techniques described in Appendix II. Taking $\lambda_o = 10^{-5}$ cm, two curves are shown for the cases $p = 0$ and $p = 1$, using the extended R.S. method as herein expounded. For $\lambda_o = 7.5 \times 10^{-6}$ cm, we show three curves, one for the extended R.S. method using $p = 1$, one for Pippard's method, and one for London's method. It is seen that the three methods are in fair agreement at lower temperatures, and

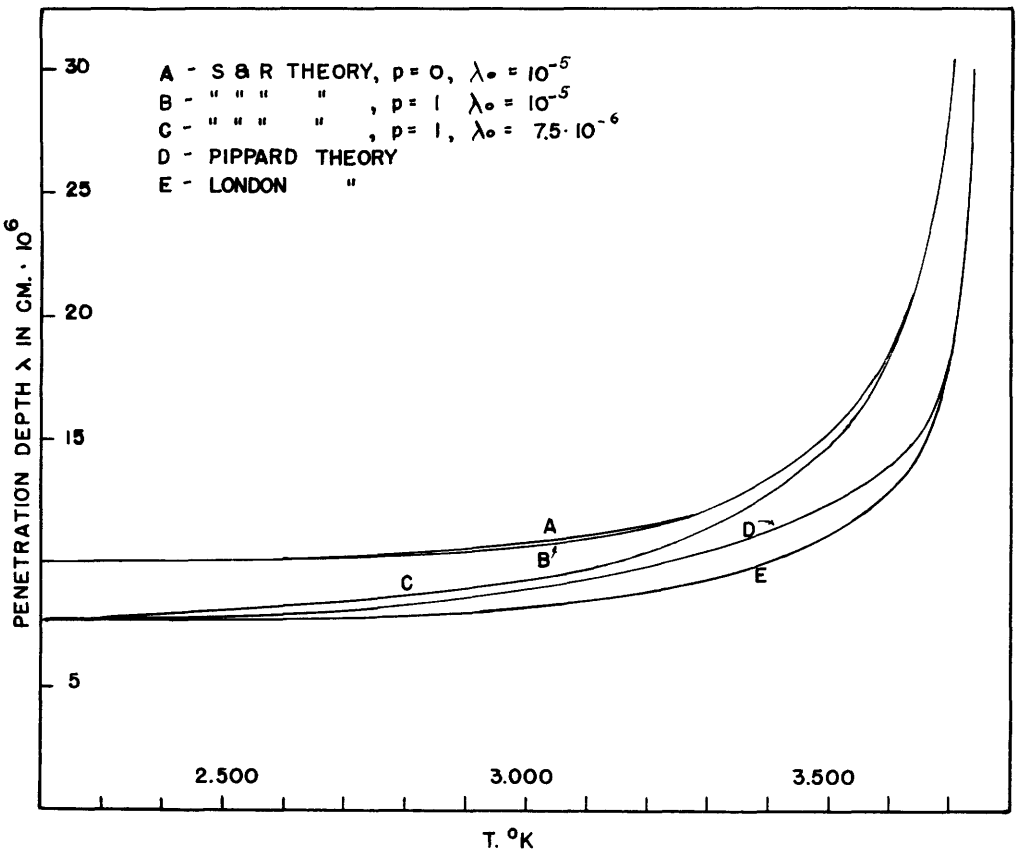

Fig. 10 Static penetration depth λ calculated from data by the methods indicated.

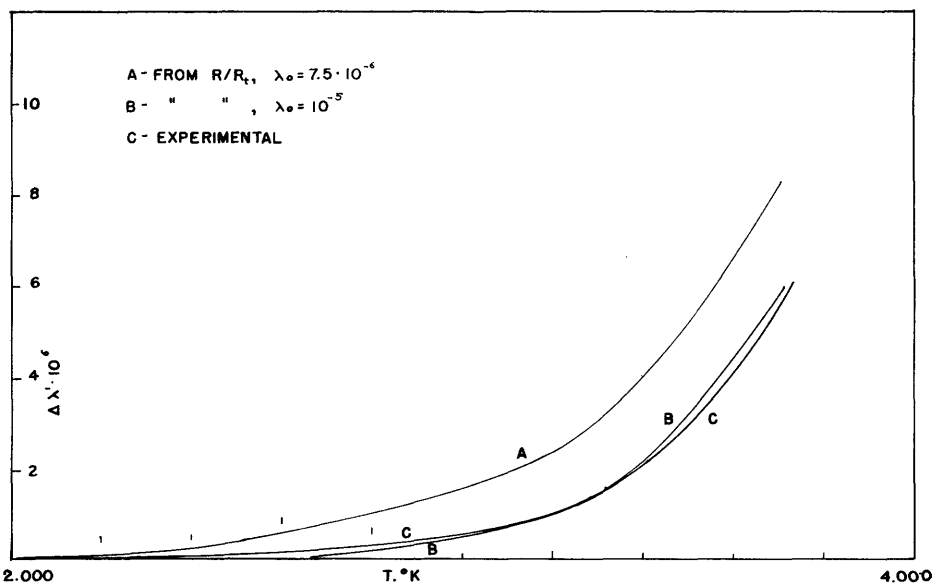

Fig. 11 Change in inductive skin depth $\Delta\lambda'$ as a function of temperature as derived from R/R_t data and from frequency shift data.

that London's and Pippard's methods are in good agreement near the transition temperature. However, these two methods yield a greater slope near the transition temperature than does the extended Reuter and Sondheimer theory.

The best choice of λ_o is determined by comparing the curves $\Delta\lambda'$, and the change in inductive skin depth, as determined from the shift in cavity resonant frequency, with these calculated from the R/R_t curve for different λ_o's. The calculated curves for $\lambda_o = 7.5 \times 10^{-6}$ and $\lambda_o = 10^{-5}$ are given in Figure 11 together with that obtained from the frequency shift data. It is seen that $\lambda_o = 10^{-5}$ cm provides a fairly good fit. Pippard's best determination of λ_o, on the other hand, was 7.5×10^{-6}.

In Figure 12 we compare our results for λ with those found by other experimenters. The comparison is made on the basis of $\Delta\lambda$, the change in penetration depth referred to 2.1°K. Pippard's data are derived from his 1200 Mc/sec frequency shift data while the other two sets of data were obtained from magnetic susceptibility measurements (13)(14). Our results appear to agree fairly well with Desirant and Shoenberg and Laurmann and Shoenberg at "high" temperatures and are somewhat closer to Pippard's at

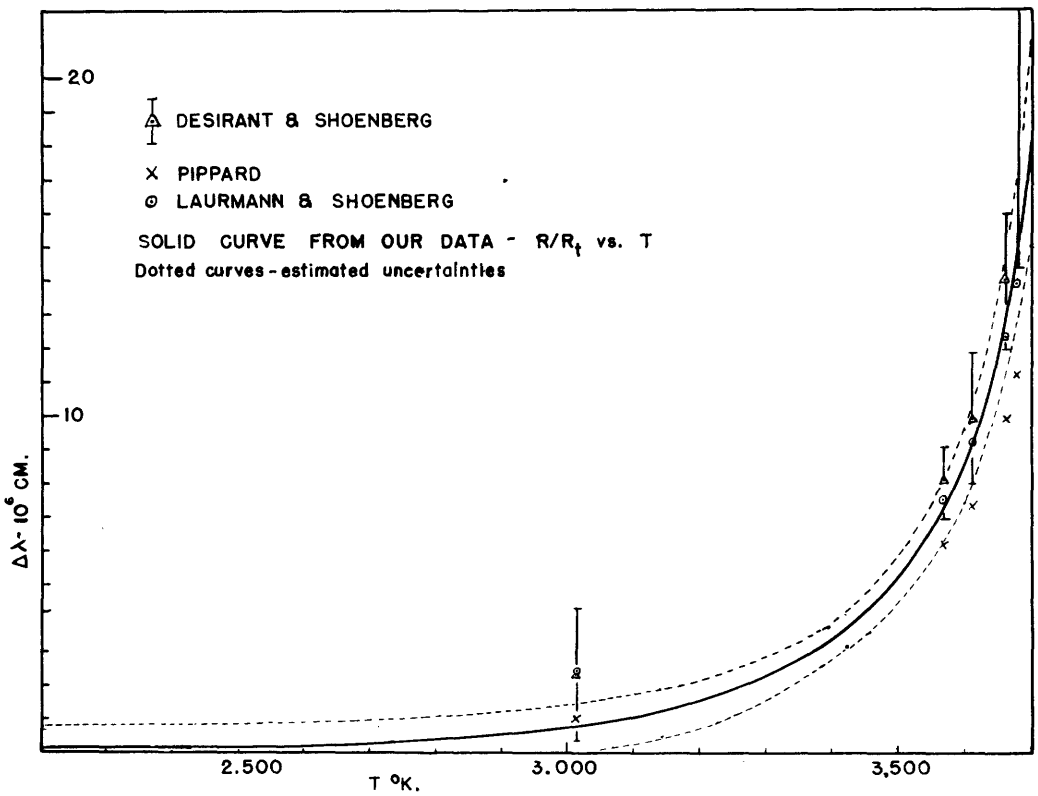

Fig. 12 Comparison of our data for $\Delta\lambda$, the change in penetration depth referred to 2.1°K with other determinations.

low temperatures. Within the specified limits of error of the data they are consistent with Desirant and Shoenberg's results over the entire range. No precision indices are available for Pippard's and Laurmann and Shoenberg's measurements.

Our data for $\Delta\lambda$ as determined from R/R_t are consistent with the calculations of ΔX_s determined from the cavity resonant frequency shift and therefore may be regarded as calculated directly from the frequency shift. From Eqs. (37) and (43) of Appendix II it is seen that this involves principally assuming the London Theory with the theory for the normal electrons entering as a second order correction. Thus, as has been pointed out (15), high frequency measurements do not furnish information about λ independently of some assumption concerning the London equations.

ACKNOWLEDGMENTS

We are greatly indebted to many of our colleagues for assistance and helpful suggestions in the course of this work. We particularly wish to acknowledge the work of Dr. John B. Garrison (now at the University of Chicago) who is jointly responsible with one of us for the development of many of the experimental techniques described and who obtained the data given for lead, and to Mr. Ralph J. Harrison of the Research Laboratory of Electronics (M.I.T.) for many valuable and illuminating discussions. We are grateful for the use of the facilities of the Research Laboratory of Electronics and the enthusiastic support of Professor J. A. Stratton and the members of the staff, particularly Messrs. R. P. Cavileer, P. Nicholas, W. B. Nowak and E. C. Ingraham.

APPENDIX I

Kinetic Derivation of Integral Formula for Current in the Normal State

The drift velocity acquired by an electron of velocity v, θ, ϕ (the polar angle θ and azimuth ϕ give the direction of motion) in moving from z_o to z in the field $E_x(z,t) = E(z)e^{i\omega t}$ arriving at time t is:

$$\dot{X}_{drift} = \frac{-\epsilon}{m} e^{i\omega t} \int_{z_o}^{z} e^{\frac{i\omega(\zeta - z)}{v \cos\theta}} E(\zeta) \frac{d\zeta}{v \cos\theta} \quad . \qquad (I\text{-}1)$$

$d\zeta/v \cos\theta$ is the time taken to traverse $d\zeta$ (along z axis); the field acting on the electron during this time is

$$E(\zeta) e^{i\omega(t - \frac{z-\zeta}{v \cos\theta})}$$

which allows for the change of field during the transit time of the electron. Such relaxation effects will later be shown negligible for cases of interest, and will be omitted in the formulas. Equation (I-1) holds for $0 \leqslant \theta \leqslant \pi$; v is assumed constant during the motion, the change due to drift velocity being neglected.

The current at z due to electrons v,θ,ϕ coming from all distances requires integration over z_o, taking account of collision losses. If dt/τ is the probability of a collision in time dt for an electron (v,θ,ϕ) then $dz/\ell \cos\theta$ is the probability of collision in traveling dz along the z axis where $\ell = v\tau$. Let Δn_o be the electrons (v,θ,ϕ) leaving z_o at t_o, and Δn the survivors which arrive at z at time t, then since

$$-d(\Delta n) = \frac{\Delta n}{\tau} dt = \frac{\Delta n dz}{\ell \cos\theta}$$

we have

$$\Delta n = \Delta n_o e^{-\frac{t-t_o}{\tau}} = \Delta n_o e^{-\frac{(z-z_o)}{\ell \cos\theta}} \quad . \qquad (I\text{-}2)$$

Evidently τ may be called the relaxation time for electrons of velocity v, and from Eq.(I-2) one easily shows τ to be the mean time between collisions, ℓ the mean free path between collisions.

In the steady state let Δn_o electrons v,θ,ϕ leave and enter each volume element $dxdydz_o$ per unit time; $\Delta n_o dz_o/\ell \cos\theta$ suffer collisions within the element, hence must be replaced by electrons thrown into v,θ,ϕ by other collisions. Of these electrons which originate at z_o

$$\frac{\Delta n_o dz_o}{\ell \cos\theta} e^{-\frac{(z-z_o)}{\ell \cos\theta}}$$

get to dz at z. We can easily check that integrating over z_o from $-\infty$ to z gives a total of Δn_o entering dz.

The average drift velocity of electrons v, θ, ϕ entering dz is found by integrating over z_o the drift velocities of electrons which originate in dz and accelerate from z_o to z, then dividing by Δn_o, the total number. For $\theta < \pi/2$ electrons may originate between z and the wall or electrons may come from the wall, either specularly reflected (fraction p or diffusely reflected (fraction $1 - p$)). The former accelerate over the entire path, the latter only from the wall to z. These are respectively the terms in Eq.(I-3). By reflecting the metal in the plane $z = 0$, and putting $E(-z) = E(z)$ reflected electrons may be considered to originate in the half space $z < 0$. Thus

$\underline{\theta < \frac{\pi}{2}}$

$$(\dot{X})_{\substack{\text{drift}\\ \text{average}}} = \frac{1}{\Delta n_o}\left(\frac{-\epsilon}{m}\right)e^{i\omega t}\left[\int_o^z e^{-\frac{(z-z_o)}{\ell\cos\theta}}\frac{\Delta n_o dz_o}{\ell\cos\theta}\int_{z_o}^z E(\zeta)e^{\frac{i\omega\tau(\zeta-z)}{\ell\cos\theta}}\frac{d\zeta}{v\cos\theta}\right.$$

$$+ p\int_{-\infty}^o e^{-\frac{(z-z_o)}{\ell\cos\theta}}\frac{\Delta n_o dz_o}{\ell\cos\theta}\int_{z_o}^z E(\zeta)e^{\frac{i\omega\tau(\zeta-z)}{\ell\cos\theta}}\frac{d\zeta}{v\cos\theta}$$

$$\left. + (1-p)\int_{-\infty}^o e^{-\frac{(z-z_o)}{\ell\cos\theta}}\frac{\Delta n_o dz_o}{\ell\cos\theta}\int_o^z E(\zeta)e^{\frac{i\omega\tau(\zeta-z)}{\ell\cos\theta}}\frac{d\zeta}{v\cos\theta}\right] \qquad (I\text{-}3)$$

$\underline{\theta > \frac{\pi}{2}}$

$$(\dot{X})_{\substack{\text{drift}\\ \text{average}}} = \frac{1}{\Delta n_o}\left(\frac{-\epsilon}{m}\right)e^{i\omega t}\int_{-\infty}^z e^{-\frac{(z-z_o)}{\ell\cos\theta}}\frac{\Delta n_o dz_o}{\ell\cos\theta}\int_{z_o}^z E(\zeta)e^{\frac{i\omega\tau(\zeta-z)}{\ell\cos\theta}}\frac{dz}{v\cos\theta}\,.$$

Integration by parts and cancellation gives

$\underline{\theta < \frac{\pi}{2}}$

$$(\dot{X})_{\substack{\text{drift}\\ \text{average}}} = \frac{-\epsilon\, e^{i\omega t}\, e^{-\frac{z}{\ell\cos\theta}(1+i\omega\tau)}}{mv\cos\theta}\left[\int_o^z dz_o e^{\frac{z_o}{\ell\cos\theta}(1+i\omega\tau)}E(z_o)\right.$$

$$\left. + p\int_{-\infty}^o dz_o\, e^{\frac{z_o}{\ell\cos\theta}(1+i\omega\tau)}E(z_o)\right]$$

$\theta > \frac{\pi}{2}$

$$(\dot{X})_{\substack{\text{drift}\\ \text{average}}} = \frac{-\epsilon\, e^{i\omega t}}{mv\cos\theta}\, e^{-\frac{z(1+i\omega\tau)}{\ell\cos\theta}} \int_{\infty}^{z} dz\; e^{\frac{z_o}{\ell\cos\theta}(1+i\omega\tau)}\, E(z_o) \quad . \quad \text{(I-4)}$$

It can be shown that $E(z_o)$ for the evaluation of Eq.(I-4) is well represented by an exponential $E(0)e^{-iKz}$ where the penetration depth $1/\mathrm{Im}(K) \sim \ell/\alpha^{1/3}$. The relaxation terms in Eq.(I-4) then enter in coefficients of the form

$$\frac{\ell\cos\theta}{z_o(1 + i\omega\tau - i K\ell\cos\theta)} \quad ;$$

hence if

$$\omega\tau \ll K\ell \sim \alpha^{1/3} \qquad \text{(I-5)}$$

the $\omega\tau$ may be dropped. This we shall do since for tin at 24×10^9 cycles/sec, $\alpha^{1/3} \cong 440$, $\omega\tau \cong 45$.

Integrate over the entire distribution, using Eq.(I-4), to obtain the total current in the metal. For the degenerate Fermi distribution, consisting of a completely filled sphere in momentum space, the above analysis of the effect of the field holds only for the electrons on the surface of the sphere.

Interior electrons are not scattered freely because the Pauli exclusion principle prevents them from going into filled states of the same momentum. The Pauli principle says that overall the interior electrons will just fill out the momentum states enclosed by the surface electron states, hence their contribution to the current is easily found. Since $(\dot{X})_{\text{drift average}}$ in Eq.(1-4) is independent of ϕ all surface electrons in a zone on the Fermi sphere in momentum space and the interior electrons will move so as to keep the zone solidly filled. The contribution to the current of the interior electrons may then be calculated as if they had a τ equal to that of the surface electrons (the corresponding ℓ would decrease as v decreases) and the same effective mass (since the shift is so small that the surface electrons remain in states of the same effective mass). This gives all electrons in a zone the same $(\dot{X})_{\text{drift average}}$ since the latter then depends only on $v_z = v\cos\theta$.

The total current is then:

$$J_x(z,t) = \int_0^{\pi} \frac{\pi(v_M \sin\theta)^2 v_M \sin\theta\, d\theta}{\frac{4}{3}\pi v_M^3} n \cdot \overset{\circ}{X}_{\substack{\text{drift} \\ \text{average}}}$$

$$= \frac{3}{4}\frac{n\epsilon^2}{mv_M} e^{i\omega t}\left[\int_0^{\pi/2} \frac{\sin^3\theta d\theta}{\cos\theta} e^{-\frac{z}{\ell\cos\theta}}\left\{\int_0^z dz\, e^{\frac{z_o}{\ell\cos\theta}} E(z_o) + p\int_{-\infty}^0 dz_o e^{\frac{-z_o}{\ell\cos\theta}} E(z_o)\right\}\right.$$

$$\left. + \int_{\pi/2}^{\pi} \frac{\sin^3\theta d\theta}{\cos\theta} e^{-\frac{z}{\ell\cos\theta}} \int_{\infty}^z dz_o e^{\frac{z_o}{\ell\cos\theta}} E(z_o)\right] \qquad \text{(I-6)}$$

where now $\ell = v_M\tau$.

Transform the integrals over θ (interchanging order of integration in Eq.(I-6)).*

$$\int_0^{\pi/2} \frac{\sin^3\theta}{\cos\theta} e^{-\frac{u}{\cos\theta}} d\theta = \int_1^{\infty} e^{-su} ds\left(\frac{1}{s} - \frac{1}{s^3}\right) = E_{i_1}(u) - E_{i_3}(u) = k(u) \qquad \text{(I-7)}$$

where $s = \frac{1}{\cos\theta}$ and in general

$$E_{i_n}(u) = \int_1^{\infty} \frac{e^{-s(u)}}{s^n} ds = E_{i_n}(-u) \quad . \qquad \text{(I-8)}$$

Eq.(I-6) becomes

$$J_x(z,t) = \frac{3}{4}\frac{n\epsilon^2}{mv_M} e^{i\omega t}\left[\int_{-\infty}^{\infty} dz_o E(z_o) k\left(\frac{z - z_o}{\ell}\right) + (1-p)\int_0^{\infty} dz_o E(z_o) k\left(\frac{z - z_o}{\ell}\right)\right]. \qquad \text{(I-9)}$$

Combine Eq.(I-9) with

$$\frac{\partial^2}{\partial z^2} E(z) e^{i\omega t} = \frac{4\pi i\omega}{c^2} J_x(z,t)$$

to give the integro-differential equation for E(z)

$$\frac{\partial^2 E}{\partial z^2} = \frac{3}{2} i\left(\frac{1}{\delta^2\ell}\right)\left[p\int_{-\infty}^{\infty} dz_o E(z_o) k\left(\frac{z - z_o}{\ell}\right) + (1-p)\int_0^{\infty} dz_o E(z_o) k\left(\frac{z - z_o}{\ell}\right)\right] \qquad \text{(I-10)}$$

*In this equation k(u) is not to be confused with the wave number k used previously in the body of the paper.

or

$$f''(x) = \alpha i \left[p \int_{-\infty}^{\infty} f(y)k(x-y)dy + (1-p) \int_{0}^{\infty} f(y)k(x-y)dy \right] \quad \text{(I-11)}$$

where

$$\alpha = \frac{3}{2} \frac{\ell^2}{\delta^2} \quad ; \quad \delta^2 = \frac{c^2}{2\pi\omega\sigma} \quad ; \quad \sigma = \frac{ne^2\ell}{mv_M} \quad \text{(I-12)}$$

and

$$f(x) = E(z) = E(\ell x) \quad . \quad \text{(I-13)}$$

Eqs.(I-9), (I-10) and (I-11) agree with the equations deduced by Reuter and Sondheimer.

If all electrons are assumed to have the same velocity v, hence lie on the surface of a sphere in momentum space, then the current is, using Eq.(I-3).

$$J_x(z,t) = \int_0^{\pi} \frac{2\pi v^2 \sin\theta \, d\theta}{4\pi v^2} \, n\dot{x}_{\text{drift average}} \quad \text{(I-14)}$$

$$= \frac{1}{2} \frac{ne^2}{mv_M} e^{i\omega t} \left[\int_0^z dz_o \frac{e^{-\left(\frac{z-z_o}{\ell}\right)}}{z-z_o} \int_{z_o}^z E(\zeta)d \; + p \int_{-\infty}^{o} dz_o \frac{e^{-\left(\frac{z-z_o}{\ell}\right)}}{z-z_o} \int_{z_o}^z E(\zeta)d\zeta \right.$$

$$\left. + (1-p) \int_{-\infty}^{o} dz_o \frac{e^{-\left(\frac{z-z_o}{\ell}\right)}}{z-z_o} \int_0^z E(\zeta)d\zeta + \int_z^{\infty} dz_o \frac{e^{-\left(\frac{z-z_o}{\ell}\right)}}{z-z_o} \int_{z_o}^z E(\zeta)d\zeta \right] \quad \text{(I-15)}$$

where the integration over θ has been done in Eq.(I-15). Equation (I-15) is Pippard's Eq.(7) p. 393 if we put $|z - z_o| = v$, $1/e = \mu$, $z = x$ and combine terms in p.

Another form of Eq.(I-15) is obtained by integration by parts which is comparable with Eq.(I-9).

It is of interest that the force of the magnetic field on the electron is much greater than that of the electric field. The ratio of forces is (making use of the space dependence e^{-iKz} for the fields) as in Eq.(5) of the main body of this paper.

$$\frac{\text{Magnetic field force}}{\text{Electric field force}} = \frac{\frac{evH}{c}}{eE} = \frac{v}{c} \frac{K}{k} = \frac{\text{electron velocity}}{\text{phase velocity of wave in the metal}}$$

$$\sim \frac{\ell}{\tau}\frac{\alpha^{1/3}}{\ell}\frac{1}{\omega} = \frac{\alpha^{1/3}}{\omega\tau} \gg 1 \qquad \text{(I-17)}$$

on substituting for K from Eq.(I-5) of this appendix. The first order effect of the magnetic field forces is merely to rotate the distribution without producing a net current, and so can be neglected.

A. Application to Direct Current Case

Equation (I-9) must apply down to the d-c case $\omega = 0$. In this case $E(z_o)$ is constant, the integrals can be evaluated, using Eq.(I-7), to give

$$J_x(z,t) = \sigma\left[1 - \tfrac{3}{4}(1-p)\left\{E_{i_2}(\tfrac{z}{\ell}) - E_{i_4}(\tfrac{z}{\ell})\right\}\right] E \qquad \text{(I-18)}$$

where

$$\sigma = \frac{ne^2\ell}{mv_M} \quad . \qquad \text{(I-19)}$$

Equation (I-18) corresponds to Fuchs' result (17) for mean free path effects in thin films, applied here to a semi-infinite metal. For $z \to \infty$, $\ell \to 0$ or $p = 1$, the conductivity given by Eq.(I-18) reduces to the ordinary bulk conductivity for direct current.

B. Expressions for the Field and Surface Impedance

Equation (I-10) has been solved (6) for the special cases $p = 0$ and $p = 1$ by methods involving the theory of Fourier Integrals. The results are given here since they will be needed for applications. (Appendix II, Eqs.(II-10)-(II-15) gives a brief outline of the simpler method applied to an extension of Eq.(I-10) to superconductors.) For $p = 1$

$$E(z) = f(x) = \frac{-2f'(0)}{\pi}\int_o^\infty \frac{\cos xt}{t^2 + i\alpha + K(t)} \; ; \; x = \frac{z}{\ell} \qquad \text{(I-20)}$$

$$\frac{f(0)}{f'(0)} = -\frac{2}{\pi}\int_o^\infty \frac{dt}{t^2 + i\alpha K(t)} \qquad \text{(I-21)}$$

$$K(t) = \frac{2}{t^3}\left\{(1+t^2)\tan^{-1} t - t\right\} \qquad \text{(I-22)}$$

Now

$$Z = \frac{4\pi i\omega\ell}{c^2}\frac{f(0)}{f'(0)} = i\sqrt{\frac{8}{3}}\,A\alpha^{1/3}\frac{f(0)}{f'(0)} \qquad \text{(I-23)}$$

where Eq.(I-23) defines A.

For $\alpha \gg 1$, Eq.(I-21) can be expanded in powers of $1/\alpha^{1/3}$, the coefficients are integrals which can be evaluated (see Appendix II, Eqs.(II-18) and (II-26)). Putting the expansion in Eq.(I-23) gives (compare Appendix II, Eq.(II-27)) in the case $p = 1$

$$Z = \frac{4\sqrt{2}A}{9\pi^{1/3}}\left[\left(1 + \frac{8\sqrt{3}}{3\pi(\pi\alpha)^{1/3}}\right) + i\left(\sqrt{3} + \frac{8}{3\pi(\pi\alpha)^{1/3}}\right)\right] \qquad \text{(I-24)}$$

$$\cong 0.4291A(1 + \sqrt{3}\, i) \quad . \qquad \text{(I-25)}$$

A table of values of Z as a function of α has been computed by Reuter and Sondheimer by numerical integration of Eq.(I-21) and is given in Table I.

At high temperatures, Z is given by the classical formula

$$Z = \frac{2\pi\omega\delta}{c^2}(1 + i) = A\alpha^{-1/6}(1 + i) \quad . \qquad \text{(I-26)}$$

Eq.(I-26) holds for both $p = 1$ and $p = 0$.

For $p = 0$ an expression for E(z) or f(x) is not available in simple form, but

$$\frac{f(0)}{f'(0)} = -\frac{1}{v + 1} \quad ; \quad v = \frac{1}{\pi}\int \ln\left(\frac{t^2 + i\alpha K(t)}{t^2 + 1}\right) dt \qquad \text{(I-27)}$$

Again Eq.(I-26) may be expanded in powers of $1/\alpha^{1/3}$ for large α, and substituting in Eq.(I-23) gives the limiting form

$$Z = \frac{A}{\sqrt{2}\pi^{1/3}}(1 + \sqrt{3}\, i) = 0.4827A\,(1 + \sqrt{3}\, i) \quad ; \quad p = 0. \qquad \text{(I-28)}$$

This is 9/8 of the value of Z for $p = 1$.

Thus far the basic constants used are n, ℓ, m, v_M; in terms of these (and ω) we have expressed τ, σ, δ, α, A. A further relation exists which expresses the momentum mv_M in terms of n. Since only the combination mv_M appears in σ, δ, α or A (but not in τ), these may be expressed as functions of n and ℓ alone.

The relation is

$$n = \frac{8\pi}{3}\frac{(mv_M)^3}{h^3}$$

which puts all electron states in one cm^3 out to maximum momentum, equal to the total number of electrons per cm^3, allowing for two spin directions. Then

$$\sigma = \frac{e^2}{h}\frac{2\pi^{1/3}}{3^{1/3}}n^{2/3}\ell \qquad \text{(I-29)}$$

$$\alpha = \frac{2\pi^{4/3}\, 3^{2/3}}{hc^2}\, \epsilon^2 \omega n^{2/3}\, \ell^3 \qquad \text{(I-30)}$$

$$A = \frac{3^{5/18}\, 2^{1/6}\, \pi^{5/9}\, h^{1/3}\, \omega^{2/3}\, n^{-2/9}}{c^{4/3}\, \epsilon^{2/3}} \qquad \text{(I-31)}$$

$$= \frac{4\pi\omega}{c^2}\sqrt{\frac{3}{8}}\,\frac{\ell}{\alpha^{1/3}} = \sqrt{\frac{2\pi\omega}{c^2}}\,\frac{\alpha^{1/6}}{\sigma^{1/2}} \qquad \text{(I-32)}$$

$$\delta = \frac{3^{1/6}}{2\pi^{2/3}}\,\frac{h^{1/2} c}{\epsilon\omega^{1/2}}\,\frac{1}{h^{1/3}\,\ell^{1/2}} \qquad \text{(I-33)}$$

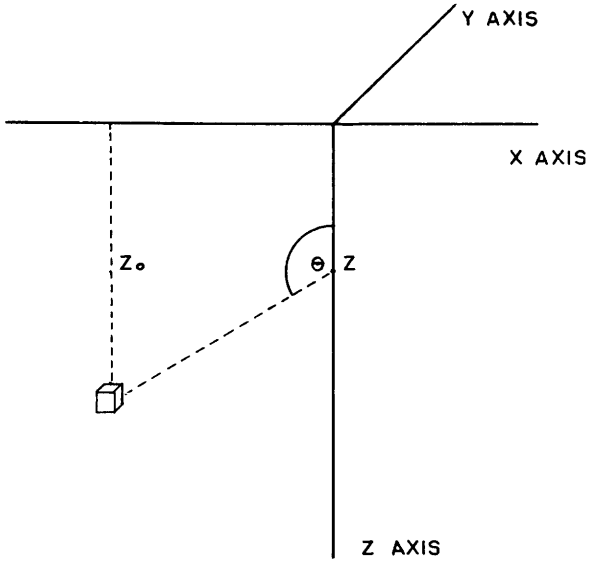

Fig. 13 Coordinate scheme.

APPENDIX II

The Surface Impedance of Metals in the Superconducting State

The measurements of surface resistance and change of surface reactance — obtained from the Q curve and resonant frequency shift of the cavity respectively — are related to the physical characteristics of the superconducting state by introducing the current of superconducting electrons (London current) into the electro-dynamic equations of Appendix I. A certain number of normal electrons are assumed to be present at each temperature. The normal electrons in the superconductor contribute to the current according to Eq.(I-6) of Appendix I, the supercurrent adds a term to this. Maxwell's equations yield a new integral equation for the field which is solved in the same way as above. The surface resistance and reactance then depend on three parameters — the resistive skin depth just above the transition δ_{et} and two quantities characteristic of the superconducting state, the static field penetration depth $\lambda(T)$ and the fraction of normal electrons which remain at any temperature, $f_N(T)$. Assumptions about the relation between the latter two parameters lead to their evaluation from the data. In particular they may both be related to single constant $\lambda_o = \lambda(0)$. The best value of λ_o is found by computing the expected change in surface reactance from the surface resistance curve as a function of T, and choosing λ_o to give best agreement with observed values of the reactance change.

It is also of interest to reduce the formulas used by London and those used by Pippard to depend on the same three parameters and thus exhibit their differences. The normal electrons were treated by different physical assumptions in their work, hence comparison of the calculated values of $\lambda(T)$ on each theory reveals the validity of their assumptions insofar as they approximate to the more accurate and more elaborate treatment given here.

A. Electrodynamic Equations for Superconductors

The field equations lead (in this one dimensional case) to the electric field-current equation

$$\frac{\partial^2 E_x}{\partial z^2} = \frac{4\pi \dot{J}}{c^2} \qquad \text{(II-1)}$$

$$J = J_N + J_s \text{ (neglecting displacement currents)} \qquad \text{(II-2)}$$

J = total current at depth in the metal
J_N = current of normal electrons
J_s = current of superconducting electrons.

Put

$$\mathring{J}_s = \frac{c^2 E_x}{4\pi\lambda^2} \tag{II-3}$$

and

$$J_N = \frac{3}{4}\,\sigma_N \ell e^{i\omega t}\left[p\int_{-\infty}^{\infty} E(t)k\left(\frac{z-t}{\ell}\right)\,dt + (1-p)\int_{0}^{\infty} E(t)k\left(\frac{z-t}{\ell}\right)\,dt \right] \tag{II-4}$$

where

$$E_x(z,t) = E(z)e^{i\omega t} \tag{II-5}$$

and k(u) is defined in Appendix I, Eq.(I-7).

$\lambda(T)$ is the static magnetic field penetration depth into the superconductor. Equation (II-3) may be interpreted as an acceleration equation for the superconducting electrons which do not collide with the lattice but accelerate under the action of the electric field in the metal at a rate determined by their inertia. When a static magnetic field is introduced, the induced electric field does the accelerating leaving behind a permanent eddy current when the steady static value is reached. This picture leads to

$$\lambda^2 = \frac{m_s c^2}{4\pi n_s c^2} \quad ,$$

but Eq.(II-3) is assumed to be more general than this specific model in which the mass and number of electrons m_s and n_s are uncertain.

Eq.(II-4) treats the normal electrons in the same way as the normal metal treatment of Appendix I, but σ_N, the equivalent d-c conductivity associated with the normal electrons will take account of the temperature dependence of the number of normal electrons.

From Eq.(II-29) of Appendix II we have

$$\sigma_N = \frac{n_N \epsilon^2 \ell}{m v_M} = \frac{\epsilon^2}{h}\,\frac{2\pi^{1/3}}{3^{1/3}}\,n_N^{2/3}\ell \quad . \tag{II-6}$$

Putting Eqs.(II-2),(II-3), and (II-4) in Eq.(II-1) and replacing E(z) by f(x) where $x = z/\ell$ gives the integro-differential equation for the field involving three parameters α, α', p,

$$f''(x) = \alpha_N i\left[p\int_{-\infty}^{\infty} f(y)k(x-y)\,dy + (1-p)\int_{0}^{\infty} k(x-y)dy \right] + \alpha' f(x) \tag{II-7}$$

$$\alpha_N = \frac{3}{2}\frac{\ell^2}{\delta_N^2} \quad , \quad \delta_N = \sqrt{\frac{c^2}{2\pi\omega\sigma_N}} \tag{II-8}$$

$$\alpha' = \frac{\ell^2}{\lambda^2} \quad . \tag{II-9}$$

Equation (II-7) can be solved in the two limiting cases p = 1 and p = 0 by a slight variation of the procedure in Appendix I. The steps are briefly outlined here; fuller discussion appears in Reuter's and Sondheimer's paper (8).

Case p = 1

$$f''(x) = i\alpha_N \int_{-\infty}^{\infty} f(y)k(x-y)\,dy + \alpha' f(y) \quad . \tag{II-10}$$

Take the Fourier transform of Eq.(II-10) with respect to x, employing the Faltung theorem, on the product of Fourier transforms and introduce a discontinuity in f'(x) at x = 0; f'(x) has been taken even in x.

$$-2\mu - t^2\,\phi(t) = i\alpha_N \phi(t)K(t) + \alpha'\phi(t) \tag{II-11}$$

where

$$\mu = f'(+0) = -f'(-0) \tag{II-12}$$

$$\phi(t) = \int_{-\infty}^{\infty} f(x)\, e^{-ixt}\, dx \tag{II-13}$$

$$K(t) = \int_{-\infty}^{\infty} k(x)\, e^{-ixt}\, dx = \frac{2}{t^3}\left\{(1+t^2)\tan^{-1} t - t\right\} . \tag{II-14}$$

Eq.(II-11) gives

$$\phi(t) = \frac{-2\mu}{t^2 + \alpha' + i\alpha_N K(t)} \quad .$$

Inverting the Fourier transform; using Eq.(II-14)

$$f(x) = \frac{1}{2\pi}\int_{-\infty}^{\infty} \phi(t)e^{ixt}\,dt = \frac{-2\mu}{\pi}\int_0^{\infty} \frac{\cos xt\,dt}{t^2 + \alpha' + i\alpha_N K(t)} \quad . \tag{II-15}$$

The surface impedance of the superconductor is given by

$$Z_s = -i\sqrt{\frac{8}{3}}\,A_N\alpha^{1/3}\,\frac{f(0)}{f'(0)} = -i\,\frac{4\pi\omega}{c^2}\,\ell\,\frac{f(0)}{f'(0)} \tag{II-16}$$

where Eq.(II-15) gives

$$\frac{f(0)}{f'(0)} = \frac{-2}{\pi}\int_0^{\infty} \frac{dt}{t^2 + \alpha' + i\alpha_N K(t)} \quad . \tag{II-17}$$

Since α_N is very large at superconducting temperatures (10^6 to 10^8), it is

useful to develop Eq.(II-17) in inverse powers of α_N, (actually $\alpha_N^{1/3}$). The first two terms are:

$$\frac{f(0)}{f'(0)} = \frac{-2}{\pi}\left[\frac{1}{(\pi\alpha_N)^{1/3}}\int_0^\infty \frac{ydy}{y^3+\beta y+i} + \frac{4i}{\pi(\pi\alpha_N)^{1/3}}\int_0^\infty \frac{dz}{(y^3+\beta y+i)^2} + O\left(\frac{1}{\pi\alpha}\right)\right] \tag{II-18}$$

where

$$\beta = \frac{\alpha'}{(\pi\alpha_N)^{2/3}} \quad . \tag{II-19}$$

The integrals in Eq.(II-18) are evaluated by partial fraction expansions to give

$$I_1(\beta) = \int_0^\infty \frac{ydy}{y^3+\beta y+i} \begin{cases} \dfrac{a^2}{1+2a^3}\left\{\pi + i\left(\dfrac{3}{2}\ln a - \dfrac{1+\frac{2}{a^3}}{\sqrt{\frac{4}{a^3}-1}}\tan^{-1}\sqrt{\dfrac{4}{a^3}-1}\right)\right\} & a \leqslant 4^{1/3} \\ \dfrac{a^2}{1+2a^3}\left\{\pi + i\left(\dfrac{3}{2}\ln a - \dfrac{\frac{1}{2}+\frac{1}{a^3}}{\sqrt{1-\frac{4}{a^3}}}\ln\dfrac{1+\sqrt{1-\frac{4}{a^3}}}{1-\sqrt{1-\frac{4}{a^3}}}\right)\right\} & a \geqslant 4^{1/3} \end{cases} \tag{II-20}$$

where a is the largest root of the cubic $x^3 - \beta x - 1 = 0$, and is given explicitly in terms of β by:

$$a = \sqrt{\frac{4\beta}{3}}\cos\left[\frac{1}{3}\cos^{-1}\frac{1}{2}\left(\frac{3}{\beta}\right)^{3/2}\right] \quad ; \quad \beta \geqslant \frac{3}{4^{1/3}} = 1.89$$

$$a = \sqrt{\frac{4\beta}{3}}\cosh\left[\frac{1}{3}\cosh^{-1}\frac{1}{2}\left(\frac{3}{\beta}\right)^{3/2}\right] \quad ; \quad \beta \leqslant \frac{3}{4^{1/3}} = 1.89 \quad . \tag{II-21}$$

The next order term in Eq.(II-18) is given by

$$I_2(\beta) = \int_0^\infty \frac{dy}{(y^3+\beta y+i)^2} = \frac{2}{3I}\left(1+\beta\frac{d}{d\beta}\right)\int_0^\infty \frac{dy}{y^3+\beta y+i} \tag{II-22}$$

where

$$I_0(\beta) = \int_0^\infty \frac{dy}{y^3+\beta y+i} = \frac{a}{1+2a^3}\left[\frac{3}{2}\ln a + \frac{3}{2\sqrt{1-\frac{4}{a^3}}}\ln\frac{1+\sqrt{1-\frac{4}{a^3}}}{1-\sqrt{1-\frac{4}{a^3}}} - \pi i\right] ; \; a^3 \geqslant 4$$

$$= \frac{a}{1+2a^3}\left[\frac{3}{2}\ln a + \frac{3}{\sqrt{\frac{4}{a^3}-1}}\tan^{-1}\sqrt{\frac{4}{a^3}-1} - \pi i\right] \quad ; \quad a^3 \leqslant 4 \tag{II-23}$$

$I_2(\beta)$

$$= \frac{-6a^3 i I_o(\beta)}{(1+2a^3)^2}\,\frac{-4ai(a^3-1)}{(1+2a^3)^2}\left[\frac{1-a^2}{4-a^3}+\frac{3}{a^3(\frac{4}{a^3}-1)}\tan^{-1}\sqrt{\frac{4}{a^3}-1}\right];\quad a^3 \leqslant 4$$

$$= \frac{-6a^3 I_o(\beta)\cdot i}{(1+2a^3)^2}\,\frac{-4ai(a^3-1)}{(1+2a^3)^2}\left[\frac{a^3-1}{a^3-4}-\frac{3}{2a^3(1-\frac{4}{a^3})^{3/2}}\ln\frac{1+\sqrt{1-\frac{4}{a^3}}}{1-\sqrt{1-\frac{4}{a^3}}}\right] a^3 \geqslant 4 \qquad \text{(II-24)}$$

and Eqs.(II-16), (II-18) give

$$Z_s = \frac{2\pi\omega}{c^2}\left(\frac{\ell}{\alpha_N^{1/3}}\right)\left(\frac{4}{\pi^{4/3}} I_1(\beta) i - \frac{16}{\pi^{8/3}}\frac{I_2(\beta)}{\alpha_N^{1/3}} \cdots\right) \quad . \qquad \text{(II-25)}$$

At the transition temperature, $\lambda = \infty$, $\beta = 0$, $a = 1$ and from Eqs.(II-20), (II-24)

$$I_1(0) = \frac{\pi}{3}(1-\frac{i}{\sqrt{3}});\quad I_2(0) = \frac{-2\pi}{9}(1+\frac{i}{\sqrt{3}}) = \frac{-2}{3} i I_o(0) \qquad \text{(II-26)}$$

$$Z_t = \frac{2\pi\omega}{c^2}\,\frac{\ell}{\alpha_t^{1/3}}\,\frac{4}{3\pi^{1/3}\sqrt{3}}\left[\left(1+\frac{8\sqrt{3}}{3\pi(\pi\alpha_t)^{1/3}}\right)+ i\left(\sqrt{3}+\frac{8}{3\pi(\pi\alpha_t)^{1/3}}\right)\right] \qquad \text{(II-27)}$$

which agrees with results of Reference 8 and Eq.(I-24) of Appendix I.

As $T \to 0$, if all electrons become superconducting, i.e. $n_N \to 0$, then $\delta_N \to 0$, $\beta \to \infty$, $a \to \infty$, $\alpha_N \to 0$. Approximations to the limiting forms of R_s and X_s may be obtained from the first term of Eq.(II-25). This gives

$$R_s = \frac{4\pi\omega\lambda^4}{c^2}\,\frac{\alpha_N}{\ell^3}\,(3\ln\beta - 1) \qquad \text{(II-29)}$$

$$X_s = \frac{4\pi\omega\lambda}{c^2}\left(1-\frac{1}{\beta^{3/2}}+\frac{5}{8\beta^3}\cdots\right) \quad . \qquad \text{(II-30)}$$

Equation (II-30) gives the correct limiting form of X_s as $T \to 0$ if all electrons become superconducting.

Putting

$$R_t = \frac{2\pi\omega\delta_{et}}{c^2} \qquad \text{(II-31)}$$

where Eq.(II-27) gives*

---

* It is assumed that $\alpha_t^{1/3} \gg 1$ and hence the second order terms in Eq.(II-27) may be dropped.

$$\delta_{et} = \frac{\ell}{\alpha_t^{1/3}} \frac{4}{3\sqrt{3}\pi^{1/3}} \qquad \begin{matrix}\text{(effective resistive}\\ \text{skin depth at the}\\ \text{transition temperature)}\end{matrix} \qquad \text{(II-32)}$$

and using

$$\frac{\alpha_N}{\alpha_t} = \frac{n_N^{2/3}}{n_t^{2/3}} = f_N^{2/3} \qquad \text{(II-33)}$$

so that Eqs.(II-31),(II-32) give

$$\frac{\alpha_N}{\ell^3} = \frac{64}{8\sqrt{3}\pi} \frac{f_N^{2/3}}{\delta_{et}^3} \qquad \text{(II-34)}$$

and

$$\beta = \frac{1}{\lambda^2\pi^{2/3}} \left(\frac{\ell}{\alpha_N^{1/3}}\right)^2 = \frac{27}{16} \frac{\delta_{et}^2}{\lambda^2 f_N^{4/9}} \qquad \text{(II-35)}$$

then Eqs.(II-29), (II-30) become, using (II-32) and (II-34), as $T \to 0$,

$$\frac{R_s}{R_t} = 0.2904 \frac{\lambda^4 f_N^{2/3}}{\delta_{et}^4} \left(3 \ln \frac{27}{16} - 1 - \ln \frac{\lambda^2 f_N^{4/9}}{\delta_{et}^2}\right) \qquad \text{(II-36)}$$

$$X_s = \frac{4\pi\omega\lambda}{c^2} \left(1 - \frac{64}{81\sqrt{3}} \frac{\lambda^3 f_N^{2/3}}{\delta_{et}^3} + \frac{5}{8}\left(\frac{4}{3\sqrt{3}}\right) \frac{\lambda^6 f_N^{4/3}}{\delta_{et}^6} \cdots\right) . \qquad \text{(II-37)}$$

More generally note that Eq.(II-25) gives:

$$\frac{R_s}{R_t} = \frac{1}{f_N^{2/9}} \frac{\mathrm{Im} I_1(\beta)}{\mathrm{Im} I_1(0)} \; ; \; \frac{X_s}{X_t} = \frac{1}{\sqrt{3}} \frac{X_s}{R_t} = \frac{1}{f_N^{2/9}} \frac{\mathrm{Re} I_1(\beta)}{\mathrm{Re} I_1(0)} . \qquad \text{(II-38)}$$

Similar expressions will now be derived for the case $p = 0$ and for London's and Pippard's treatments.

Case $p = 0$

$$f''(x) + \alpha_N i \int_0^\infty f(y)\, k(x - y)\, dy + \alpha' f(x) . \qquad \text{(II-39)}$$

The more complicated manipulation which leads to a solution of this Wiener-Hopf type integral equation is given by Reuter and Sondheimer and is too long to outline here. The procedure, which follows that of Wiener and Hopf, introduces a function equal to the difference of the two sides of Eq.(II-39) for $X < 0$, but zero for $X > 0$, takes the Laplace Transform of

this function again using the Faltung theorem, discusses the regions of existence of the various transforms and separates the transform equation into a side which is regular in the left half plane and a side regular in the right half plane with an overlapping region of regularity. The two sides therefore determine an integral function; determining the asymptotic behavior of this integral function identifies the integral function and thence the transform of f(x). The ratio f(0)/f'(0) is then expressed in terms of the transform and found explicitly. The modification introduced by the term $\alpha f'(x)$ in Eq.(II-39) is to alter the characteristic equation whose roots must be located to separate the transform equation properly. We now find for $\alpha' > 1$, the characteristic equation has no roots in the strip $-1 \leqslant \text{Res} \leqslant 1$ for all X, s is the transform variable,

$$F(s) = \int_{-\infty}^{\infty} e^{-xs} f(x)\, dx \quad .$$

We finally find the quantity of interest in the form

$$\frac{f(0)}{f'(0)} = \frac{-1}{\upsilon + 1} \; ; \quad \upsilon = \frac{1}{\pi} \int_0^{\infty} \ln \left(\frac{t^2 + \alpha' + i\alpha_N K(t)}{t^2 + 1} \, dt \right) \qquad \text{(II-40)}$$

where

$$K(t) = \frac{2}{t^3} \left\{ (1 + t^2) \tan^{-1} t - t \right\} \quad . \qquad \text{(II-41)}$$

Integrate Eq.(II-40) by parts, put $K(t) \sim \frac{\pi}{t}$ and get,

$$\upsilon + 1 = \frac{2i\alpha_N}{\pi} \int_0^{\infty} \frac{\left(\frac{3\pi}{2t} + \frac{\alpha'}{i\alpha_N}\right)}{t^2 + \alpha' + i\frac{\alpha_N \pi}{t}} \, dt \qquad \text{(II-42)}$$

$$= \frac{3i(\alpha_N \pi)^{1/3}}{\pi} \int_0^{\infty} \frac{dy}{y^3 + \beta y + i} + \frac{2\alpha'}{\pi(\pi\alpha_N)^{1/3}} \int_0^{\infty} \frac{y\,dy}{y^3 + \beta y + i}$$

$$= \frac{3}{4} i(\pi\alpha_N)^{1/3} \left[I_0(\beta) - \frac{2}{3} i\beta I_1(\beta) \right] \quad .$$

From Eqs.(II-16),(II-40),(II-42) we get

$$Z_s = \frac{4\pi\omega\ell}{c^2} \frac{\pi}{3(\pi\alpha_N)^{1/3}} \frac{1}{\left[I_0(\beta) - \frac{2}{3} i\beta I_1(\beta) \right]} \quad . \qquad \text{(II-43)}$$

Equation (II-43) corresponds to the first term of Eq.(II-25).

At $T = T_t$, $\beta = 0$, using Eq.(II-26), Eq.(II-43) becomes

$$Z_t = \frac{2\pi\omega}{c^2}\frac{\ell}{\alpha_t^{1/3}}\frac{\sqrt{3}}{2\pi^{1/3}}(1 + i\sqrt{3}) \qquad (p = 0) \quad . \qquad \text{(II-44)}$$

Again as in the case of Eqs.(II-29) and (II-30), as $T \to 0$, $\beta \to \infty$

$$I_o(\beta) \to \frac{3}{2}\frac{\ln\beta}{\beta} - \frac{\pi i}{2\beta} \quad . \qquad \text{(II-45)}$$

Then Eq.(II-45) in Eq.(II-43) with Eqs.(II-19 and (II-9) give, as $T \to 0$,

$$Z_s = \frac{4\pi\omega}{c^2}\frac{\pi}{3}\frac{\ell}{(\pi\alpha)^{1/3}}\left(\frac{1}{\frac{-2}{3}\,i\beta\frac{\pi}{2\beta^{1/2}}}\right) = \frac{4\pi i\omega}{c^2}\frac{\ell}{(\pi\alpha)^{1/3}}\frac{1}{\beta^{1/2}} = \frac{4\pi i\omega\lambda}{c^2} \qquad \text{(II-46)}$$

which agrees with Eq.(II-30).

Note that Eqs.(II-44) and (II-32) lead to

$$\delta_{et} = \frac{\ell}{\alpha_t^{1/3}}\frac{\sqrt{3}}{2\pi^{1/3}} \qquad \text{(II-47)}$$

hence as in Eq.(II-35), using Eq.(II-33)

$$\beta = \frac{1}{\lambda^2\pi^{2/3}f_N^{4/9}}\left(\frac{\ell}{\alpha_t^{1/3}}\right)^2 = \frac{4}{3}\frac{\delta_{et}^{\,2}}{\lambda^2 f_N^{4/9}} \qquad (p = 0) \qquad \text{(II-48)}$$

and, as in Eq.(II-34),

$$\frac{\ell}{\alpha_N^{1/3}} = \frac{2\pi^{1/3}}{\sqrt{3}}\frac{\delta_{et}}{f_N^{2/9}} \quad . \qquad \text{(II-49)}$$

Pippard's Treatment

This differs from the above in treating the current due to the normal electrons by means of an effective conductivity derived from the ineffectiveness concept.

$$Z = \frac{-4\pi i\omega}{c^2}\frac{E(0)}{\frac{\partial E(0)}{\partial z}} \quad \text{(equivalent to (II-16))} \quad . \qquad \text{(II-50)}$$

From Eqs.(II-1),(II-2)

$$\frac{\partial^2 E}{\partial z^2} = \frac{4\pi\mathring{J}}{c^2} \quad ; \quad \mathring{J} = \mathring{J}_s + \mathring{J}_N = \frac{c^2 E}{4\pi\lambda^2} + \sigma_e\mathring{E} \quad . \qquad \text{(II-51)}$$

The effective conductivity

$$\sigma_e = \frac{\delta_s}{\ell}\sigma_N \qquad \text{(II-52)}$$

is assumed to be a fraction δ_s/ℓ smaller than the d-c conductivity of the normal electrons (using the "ineffectiveness concept"). Here δ_s is the

penetration depth of the field into the superconductor.

Since J(z) is now proportional to E(z)(for harmonic time dependence $e^{i\omega t}$), Eq.(II-51) leads to a wave equation for E. Putting

$$E(z) = E_o e^{-iKz} \tag{II-53}$$

$$K^2 = -\left(\frac{1}{\lambda^2} + \frac{4\pi i\omega\sigma_e}{c^2}\right) = -\left(\frac{1}{\lambda^2} + \frac{2i}{\delta_e^2}\right) . \tag{II-54}$$

Therefore

$$\begin{aligned} K &= K_r + iK_i \\ K_r &= \frac{1}{\lambda}\sqrt{\frac{q-1}{2}} \\ K_i &= -\frac{1}{\lambda}\sqrt{\frac{q+1}{2}} \\ q &= \sqrt{1 + \frac{4\lambda^4}{\delta_e^4}} \quad . \end{aligned} \tag{II-55}$$

From Eqs.(II-50),(II-53),(II-55)

$$Z_s = \frac{4\pi\omega}{c^2}\frac{1}{K} = \frac{4\pi\omega}{c^2}\lambda\left[\frac{1}{q}\sqrt{\frac{q-1}{2}} + \frac{i}{q}\sqrt{\frac{q+1}{2}}\right] . \tag{II-56}$$

Now

$$\frac{\delta_e^2}{\delta_{et}^2} = \frac{\sigma_{et}}{\sigma_e} = \frac{\frac{\delta_{et}}{\ell}\sigma_{Nt}}{\frac{\delta_s}{\ell}\sigma_N} = \frac{\delta_{et}}{\delta_s}\frac{1}{f_N^{2/3}} \quad . \tag{II-57}$$

This assumes ℓ is constant, i.e. the d-c conductivity in presence of a magnetic field greater than critical is constant. Hence using Eq.(II-55)

$$\frac{f_N^{2/3}}{\delta_{et}^3} = \frac{1}{\delta_s}\frac{1}{\delta_e^2} = \frac{-K_i}{\delta_e^2} = \frac{1}{\lambda}\sqrt{\frac{q+1}{2}}\sqrt{\frac{q^2-1}{2\lambda^2}}$$

or

$$(q+1)(q^2-1) = \frac{8\lambda^6 f_N^{4/3}}{\delta_{et}^6} \quad . \tag{II-58}$$

As $T \to 0$, $q \to 1$, and Eq.(II-58) may be solved for q as an expansion in powers of

$$\frac{2\lambda^6 f_N}{\delta_{et}^6} \quad .$$

Then any function of q may be expanded similarly. Thus

$$R_s = \frac{4\pi\omega\lambda}{c^2}\sqrt{\frac{q-1}{2q^2}} \tag{II-59}$$

$$= \frac{4\pi\omega\lambda}{c^2}\frac{\lambda^3 f_N^{3/2}}{\delta_{et}^3}\left(1 - 3\left(\frac{\lambda}{\delta_{et}}\right)^6 f_N^{4/3} + 13\left(\frac{\lambda}{\delta_{et}}\right)^{12} f_N^{8/3} - 64\left(\frac{\lambda}{\delta_{et}}\right)^{18} f_N^4 \cdots\right).$$

Noting

$$R_t = \frac{2\pi\omega\delta_{et}}{c^2} \tag{II-60}$$

$$\frac{R_s}{R_t} = \frac{2\lambda^4 f_N^{2/3}}{\delta_{et}^4}\left(1 - 3\left(\frac{\lambda}{\delta_{et}} f_N^{2/9}\right)^6 + 13\left(\frac{\lambda}{\delta_{et}} f_N^{2/9}\right)^{12} - 64\left(\frac{\lambda}{\delta_{et}} f_N^{2/9}\right)^{18} \cdots\right) \tag{II-61}$$

$$X_s = \frac{4\pi\omega\lambda}{c^2}\sqrt{\frac{q+1}{2q^2}} \tag{II-62}$$

$$= \frac{4\pi\omega\lambda}{c^2}\left(1 - \frac{3}{2}\left(\frac{\lambda}{\delta_{et}} f_N^{2/9}\right)^6 + \frac{47}{8}\left(\frac{\lambda}{\delta_{et}} f_N^{2/9}\right)^{12} - \frac{443}{16}\left(\frac{\lambda}{\delta_{et}} f_N^{2/9}\right)^{18} \cdots\right).$$

It is of interest to compare Eq.(II-61) with the approximate expression obtained by Pippard

$$\frac{R_s}{R_t} = \frac{2\left(\frac{\lambda}{\delta_{et}}\right)^4 f_N^{2/3}}{\left[1 + 6 f_N^{4/3}\left(\frac{\lambda}{\delta_{et}}\right)^6\right]^{1/2}} \tag{II-63}$$

$$= 2\left(\frac{\lambda}{\delta_{et}}\right)^4 f_N^{2/3}\left[1 - 3\left(\frac{\lambda}{\delta_{et}} f_N^{2/9}\right)^6 + \frac{27}{2}\left(\frac{\lambda}{\delta_{et}} f_N^{2/9}\right)^{12} - \frac{135}{2}\left(\frac{\lambda}{\delta_{et}} f_N^{2/9}\right)^{18} \cdots\right].$$

Also the correction factor for normal electrons in Eq.(II-62), which Pippard evaluates in terms of the ratio $r = R_s/R_t$, may be rigorously expanded in terms of r and f_N.

$$\sqrt{\frac{q+1}{2q^2}} = 1 - 0.5304\, f_N^{1/3} r^{3/2} - 0.1094\, f_N^{2/3} r^3 \cdots \quad . \tag{II-64}$$

Pippard takes $f_N = 1$, since the terms in r are small when $f_N \neq 1$, but near the transition where the correction factor differs from 1, $f_N = 1$. Note that f_N here differs from Pippard because he takes the conductivity proportional to n_N whereas we use $n_N^{2/3}$ corresponding to a degenerate Fermi gas of electrons.

London's Treatment

The normal electrons are now treated as having an effective a-c

conductivity (smaller than the d-c conductivity) which is assumed to vary as $n_N^{2/3}$ but not with the penetration depth of the field (i.e. no "ineffectiveness concept" is used). As in Pippard's treatment Eqs.(II-50),(II-51),(II-53),(II-54),(II-55),(II-56) hold but not (II-52) or (II-57). Instead we have

$$\frac{\delta_e^2}{\delta_{et}^2} = \frac{\sigma_{et}}{\sigma_e} = \frac{1}{f_N^{2/3}} \quad . \tag{II-65}$$

Hence

$$q = \sqrt{1 + \frac{4\lambda^4}{\delta_e^4}} = \sqrt{1 + \frac{4\lambda^4}{\delta_{et}^4} f_N^{4/3}} \tag{II-66}$$

$$\frac{R_s}{R_t} = \frac{2\lambda}{\delta_{et}} \sqrt{\frac{q-1}{2q^2}} = \frac{2\lambda^3 f_N^{2/3}}{\delta_{et}^3} \left[1 - \frac{5}{2} \left(\frac{\lambda f_N^{1/3}}{\delta_{et}} \right)^4 - \frac{71}{8} \left(\frac{\lambda}{\delta_{et}} f_N^{1/3} \right)^8 \cdots \right] \tag{II-67}$$

$$X_s = \frac{4\pi\omega\lambda}{c^2} \sqrt{\frac{q+1}{2q^2}} = \frac{4\pi\omega\lambda}{c^2} \left[1 - \frac{3}{2} \left(\frac{\lambda}{\delta_{et}} f_N^{1/3} \right)^4 + \frac{35}{8} \left(\frac{\lambda}{\delta_{et}} f_N^{1/3} \right)^8 \cdots \right] \tag{II-68}$$

1. Calculation Procedures

The experimental data consist of R_s/R_t as a function of T, the absolute value of R_t, and the change in X_s from the transition temperature down. The theory can be applied to the data in several ways. λ can be found as a function of T if f_N is known, or if a relation is assumed between f_N and λ. The most reasonable relation in the light of present theories relates f_N and λ but introduces the constant λ_o, the value of λ when all electrons are superconducting. By using the $\Delta X_s(T)$ data also, λ_o can then be fixed. In addition the theory gives some simple quantitative relations which can be checked on the data; namely the frequency dependence of the initial slope of the resistance curve and of the resistance at temperatures well below the transition, and the slope of the reactance curve (or inductive skin depth curve) at T_t.

To relate f_N and λ, put

$$n_N + n_s = n_o \tag{II-69}$$

(where n_o is number of normal electrons at the transition temperature).

$$\frac{\lambda^2}{\lambda_o^2} = \frac{n_o}{n_s} \quad . \tag{II-70}$$

Equations (II-69) and (II-70) give

$$f_N = \frac{n_N}{n_o} = 1 - \frac{n_s}{n_o} = 1 - \frac{\lambda_o^2}{\lambda^2} \quad . \tag{II-71}$$

Equation (II-69) is part of the "two fluid" assumption about electrons in superconductors, the constant total is divided between superconducting and normal electrons which behave independently. Equation (II-70) is based on the acceleration picture of superconducting electrons with inertia but no resistance; then

$$\lambda^2 = \frac{m_s c^2}{4\pi n_s \epsilon^2} \quad .$$

The mass m_s is unknown; even though superconducting electrons do not interact with lattice vibrations there is no reason to think the potential field of the crystal does not affect the mass.

Calculation of $\lambda(T)$ using the extended theory of Reuter and Sondheimer to treat the normal electrons is then based on the equations

p = 1

$$\frac{R_s}{R_t} = \frac{1}{f_N^{2/9}} \frac{\mathrm{Im}I_1(\beta)}{\mathrm{Im}I_1(0)} \quad ; \quad f_N = 1 - \frac{\lambda_o^2}{\lambda^2}$$

$$\beta = \frac{27}{16} \frac{\delta_{et}^2}{\lambda^2 f_N^{4/9}} \qquad I_1(\beta) \text{ is given in Eqs. (II-20,(II-21)}$$

$$\delta_{et}^2 = \frac{c^2 R_t}{2\pi\omega} \tag{II-72}$$

$$\frac{c^2 X_s}{4\pi\omega} = \delta_{et} \frac{\sqrt{3}}{2} \frac{\mathrm{Re}I_1(\beta)}{f_N^{2/9}\mathrm{Re}I_1(0)} \quad ; \quad \frac{c^2}{4\pi\omega} X_t = \delta_{et} \frac{\sqrt{3}}{2} \quad .$$

The procedure is to choose λ_o, calculate $f_N(\lambda)$, $\beta(\lambda)$, using the known value of R_t to find δ_{et}, $R_s/R_t(\lambda)$ using tables of $\mathrm{Im}I_1(\beta)$, hence from $R_s/R_t(T)$ find $\lambda(T)$. From tables of $\mathrm{Re}I_1(\beta)$, the inductive skin depth

$$\frac{c^2 X_s(\lambda)}{4\pi\omega}$$

is found, hence

$$\frac{c^2 X_s(T)}{4\pi\omega}$$

from $\lambda(T)$.

The values of

$$\frac{c^2}{4\pi\omega}\left[X_s(T) - X_s(T_t)\right]$$

are compared with experimental values found from the frequency shift of the cavity. λ_o is adjusted for best fit of the reactance data.

Case p = 0

$$\frac{R_s}{R_t} = \frac{1}{f_N^{2/9}} \frac{\mathrm{Re}I_3(\beta)}{\mathrm{Re}I_3(0)} \left|\frac{I_3(0)}{I_3(\beta)}\right|^2 \quad ; \quad I_3(\beta) = I_o(\beta) - \frac{2}{3} i\beta I_1(\beta)$$

$$\beta = \frac{4}{3} \frac{\delta_{et}^2}{\lambda^2 f_N^{4/9}}$$

$$\delta_{et} = \frac{c^2 R_t}{2\pi\omega} \tag{II-73}$$

$$\frac{c^2 X_s}{4\pi\omega} = \delta_{et} \frac{\sqrt{3}}{2} \frac{\mathrm{Im}I_3(\beta)}{\mathrm{Im}I_3(0)} \left|\frac{I_3(0)}{I_3(\beta)}\right|^2 .$$

Calculations based on Pippard's equations use:

$$\frac{R_s}{R_t} = \frac{\lambda}{\delta_{et}} \frac{\sqrt{2(q-1)}}{q} \quad ; \quad f_N = 1 - \frac{\lambda_o^2}{\lambda^2}$$

$$q^2 = 1 + \frac{8\lambda^6 f_N^{4/3}}{\delta_{et}^6} \frac{1}{q+1} .$$

As above λ_o is chosen, $f_N(\lambda)$ found, $q(\lambda)$ found by solving the cubic for q using the known value of δ_{et}. Hence we find $R_s/R_t(\lambda)$ and then from $R_s/R_t(T)$, $\lambda(T)$ is found. The $\lambda(T)$ and $q(\lambda)$ then lead to $c^2X_s/4\pi\omega$. The cubic in q is quickly solved by tabulating or plotting the root as a function of the single parameter, Newton's rule can be used to improve a first guess. (The desired root is unity when $f_N = 0$.) Various λ_o's may then be tried to fit the reactance data best.

Calculations on London's equations use the same equations as above except for the one giving q. This becomes

$$q = \sqrt{1 + \frac{4\lambda^4}{\delta_{et}^4} f_N^{4/3}} \tag{II-75}$$

2. Initial Slopes

The frequency dependence of the initial slope of $\frac{R_s}{R_t}(T)$ is found from Eqs.(II-38),(II-20),(II-35), (for the case p = 1).

$$\left[\frac{d}{dT}\frac{R_s}{R_t}(T)\right]_{T=T_t} = -\frac{2}{9}\frac{\frac{R_s}{R_t}(T)}{T_t}\left(\frac{df_N}{dT}\right)_{T=T_t} + \left[\frac{1}{f_N^{2/9}}\frac{d}{d\beta}\left(\frac{ImI_1(\beta)}{ImI_1(0)}\right)\frac{d\beta}{dT}\right]_{T=T_t} \tag{II-76}$$

$$= \left(\frac{2}{9} - \frac{27}{16}\frac{\sqrt{3}}{\pi}\frac{\delta_{et}^2}{\lambda_o^2}\right)\frac{1}{n_o}\left(\frac{dn_s}{dT}\right)_{T=T_t}$$

using

$$\frac{d}{dT}\frac{\lambda_o^2}{\lambda^2} = \frac{1}{n_o}\frac{dn_s}{dT}$$

and

$$\frac{df_N}{dT} = -\frac{d}{dT}\left(\frac{\lambda_o^2}{\lambda^2}\right); \quad \frac{d\beta}{dT} = \frac{27}{16}\delta_{et}^2\frac{d}{dT}\left(\frac{1}{\lambda^2}\right)$$

The 2/9 term in Eq.(II-76) is only a few percent of the other term in the case of interest and since

$$\frac{dn_s}{dT} < 0, \quad \frac{d}{dT}\frac{R_s}{R_t}(T) > 0 \quad .$$

Moreover, since

$$\delta_{et} = \frac{4}{3\sqrt{3\pi}^{1/3}}\frac{\ell}{\alpha_t^{1/3}} \quad \text{and} \quad \alpha = \frac{2\pi^{4/3}}{hc^2}\epsilon^2\omega n^{2/3}\ell^3 \quad ,$$

the frequency dependence of the initial slope is closely $1/\omega^{2/3}$.

The initial slope of the inductive skin depth $c^2X_s/4\pi\omega$ is similarly found to be

$$\frac{d}{dT}\frac{c^2X_s}{4\pi\omega} = \frac{\sqrt{3}}{9}\delta_{et}\frac{1}{n_o}\left(\frac{dn_s}{dT}\right)_{T=T_t} \tag{II-77}$$

which is negative. Since $c^2X_s/4\pi\omega$ at lower temperatures decreases to λ_o, the curve goes through a maximum near T_t. At higher frequencies, however, we may have $\delta_{et} \lesssim \lambda_o$ and the character of the curve will change.

Well below the transition, the limiting value of R_s/R_t has the form given by Eq.(II-36).

APPENDIX III

Table of Nomenclature

$E_x(z,t)$ = electric field in x direction

$E(z)$ = space amplitude of $E_x(z,t)$

J, J_x = total current in metal

J_N = current carried by normal electrons

J_s = current carried by superconducting electrons

$Z = R + iX$ = surface impedance of metal

R = surface resistance ($= \frac{1}{\Sigma}$ in Pippard's notation)

X = surface reactance

Z_t, R_t, X_t = values of Z,R,X at transition temperature

Z_s, R_s, X_s = values of Z,R,X in superconducting state

σ, σ_N = d-c conductivity of normal electrons (above transition use σ)

σ_E = effective a-c conductivity

δ, $\delta_N = \sqrt{\frac{c^2}{2\pi\omega\sigma_N}}$ = classical penetration depth from d-c conductivity of normal electrons (above transition use δ)

$\delta_{et} = \frac{c^2 R_t}{2\pi\omega}$ = effective value of resistive skin depth

δ_s = penetration depth of field in superconductor ($= -\frac{1}{K_1}$ in Pippard's or London's treatments)

$\lambda(T)$ = penetration depth of static magnetic field

$k = \frac{\omega}{c}$ = propagation constant for free space

$K = K_r + iK_1$ = propagation constant of field in superconductor

ℓ = mean free path of electrons

p = fraction of electrons specularly reflected at the surface

$f_N(T)$ = fraction of electrons which are normal in the superconductor

n_s = number of superconducting electrons per cc.

m_s = mass of superconducting electrons

n, n_N = number of normal electrons per cc. (above transition use n)

α, $\alpha_N = \frac{3}{2}\frac{\ell^2}{\delta_N^2}$ = dimensionless constant characterising normal and superconducting states (above transition use α)

$\alpha' = \frac{\ell^2}{\lambda^2}$ = dimensionless constant characterizing superconducting state

$\beta = \frac{\alpha'}{(\pi\alpha)^{2/3}}$

$A, A_N = \frac{4\pi\omega}{c^2}\sqrt{\frac{3}{8}}\left(\frac{2}{3}\right)^{1/3} \ell^{1/3}\, \delta_N^{2/3}$ (above transition use A)

v = electron velocity

v_M = maximum velocity of Fermi distribution

τ = mean time between collisions

$\dot{X}_{drift}$ = drift velocity in x direction acquired by electron

$\dot{X}_{drift\ average}$ = average value of $(\dot{X})_{drift}$ for electrons from all directions

q = parameter used in Pippard and London treatment (Pippard uses m)

$$I_o(\beta) = \int_o^\infty \frac{dy}{y^3 + \beta y + 1}$$

$$I_1(\beta) = \int_o^\infty \frac{y\,dy}{y^3 + \beta y + 1}$$

$$I_2(\beta) = \int_o^\infty \frac{dy}{(y^3 + \beta y + 1)^2}$$

$$I_3(\beta) = I_o(\beta) - \frac{2}{3} i\beta I_1(\beta)$$

APPENDIX IV

NUMERICAL TABLES

Table I

Surface Impedance as a Function of α
(Reuter and Sondheimer)

	A/R		A/X	
	p = 1	p = 0	p = 1	p = 0
0.01	---	0.464	---	0.452
0.25	0.804	0.782	0.773	0.703
3	1.222	1.117	1.038	0.885
20	1.585	1.374	1.177	0.991
100	1.845	1.562	1.247	1.056
700	2.062	1.741	1.294	1.110
4×10^3	2.177	1.852	1.317	1.141
5×10^4	2.264	1.956	1.333	1.169
3×10^5	2.296	2.000	1.339	1.180
∞	2.330	2.071	1.345	1.196

Table II

Numerical Values of the Integrals Used in Calculations of Appendix II

β	$\mathrm{Re}I_1(\beta)$	$\mathrm{Im}I_1(\beta)$	$\mathrm{Re}\frac{I_1(\beta)}{I_1(0)}$	$\mathrm{Im}\frac{I_1(\beta)}{I_1(0)}$	$\mathrm{Re}I_3(\beta)$	$\mathrm{Im}I_3(\beta)$	$\frac{\mathrm{Re}I_3(\beta)}{\mathrm{Re}I_3(0)}\left[\frac{I_3(0)}{I_3(\beta)}\right]^2$	$\frac{\mathrm{Im}I_3(\beta)}{\mathrm{Im}I_3(0)}\left[\frac{I_3(0)}{I_3(\beta)}\right]^2$
0.0	1.0472	−0.6046	1.0000	1.0000	0.6046	−1.0472	1.0000	1.0000
0.2	1.0430	−0.5408	0.9960	0.8945	0.5665	−1.1169	0.8735	0.9943
0.4	1.0317	−0.4832	0.9852	0.7992	0.5323	−1.1860	0.7618	0.9799
0.6	1.0157	−0.4321	0.9699	0.7147	0.5019	−1.2542	0.6651	0.9596
0.8	0.9965	−0.3873	0.9516	0.6406	0.4745	−1.3213	0.5822	0.9360
1.0	0.9758	−0.3481	0.9318	0.5758	0.4502	−1.3872	0.5119	0.9106
1.4	0.9321	−0.2841	0.8901	0.4699	0.4081	−1.5145	0.4011	0.8595
1.8	0.8891	−0.2352	0.8490	0.3890	0.3738	−1.6362	0.3209	0.8110
2.0	0.8683	−0.2152	0.8292	0.3560	0.3586	−1.6943	0.2892	0.7888
2.2	0.8485	−0.1976	0.8103	0.3268	0.3450	−1.7519	0.2617	0.7672
3.0	0.7772	−0.1449	0.7422	0.2397	0.2997	−1.9680	0.1829	0.6934
4.0	0.7056	−0.1042	0.6738	0.1723	0.2589	−2.2152	0.1259	0.6218
6.0	0.6026	−0.0618	0.5754	0.1022	0.2053	−2.6487	0.0703	0.5240
8.0	0.5328	−0.0412	0.5088	0.0681	0.1720	−3.0260	0.0453	0.4599
10.0	0.4822	−0.0297	0.4605	0.0491	0.1484	−3.3649	0.0316	0.4141
15.0	0.3988	−0.0159	0.3808	0.0263	0.1121	−4.0901	0.0162	0.3411
20.0	0.3475	−0.0101	0.3318	0.0167	0.0902	−4.7106	0.0098	0.2963
25.0	0.3123	−0.0070	0.2982	0.0116	0.0769	−5.2672	0.0067	0.2650

Table III

Smoothed Values of the Surface Resistance of Sn
In The Normal State at 24,000 Mc/sec.

T	R (ohms)
300	0.1217
200	0.0995
140	0.08014
100	0.0636
80	0.0532
70	0.0478
60	0.0420
50	0.0358
40	0.0293
35	0.0260
30	0.0227
25	0.0198
20	0.0180
15	0.0175
10	0.0175
5	0.0175
4.2	0.0175

Table IV

Smoothed Values of R/Rt — Normalized Surface Resistance of Sn in Superconducting State at 24,000 Mc/sec

T°K	R/R_t
3.751	1.000
3.740	0.932
3.730	0.860
3.720	0.806
3.710	0.749
3.700	0.702
3.680	0.627
3.660	0.569
3.630	0.498
3.600	0.444
3.500	0.319
3.400	0.247
3.300	0.198
3.200	0.171
3.000	0.142
2.800	0.120
2.600	0.109
2.400	0.103
2.100	0.097

REFERENCES

(1) F. Bitter, J. B. Garrison, J. Halpern, E. Maxwell, J. C. Slater and C. F. Squire, Phys. Rev. 70, 97 (1946).

(2) E. Maxwell, P. M. Marcus and J. C. Slater, Am. Phys. Soc. Bul. 23, (1948).

(3) M.I.T., R.L.E. Quarterly Progress Reports (1946 to 1948).

(4) H. London, Proc. Roy. Soc. A176, 522 (1940).

(5) J. G. Daunt, T. C. Keeley and K. Mendelssohn, Phil. Mag. 23, 264 (1937).

(6) S. C. Collins, Phys. Rev. 70, 98 (1946); Rev. Sci. Inst. 18, 157 (1947).

(7) A. B. Pippard, Proc. Roy. Soc. A191, 370 (1947).

(8) G. E. H. Reuter and E. H. Sondheimer, Proc. Roy. Soc. A195, 336 (1948).

(9) S. A. Schelkunoff, Electromagnetic Waves, Van Nostrand, New York (1943).

(10) J. C. Slater, Rev. Mod. Phys. 18, 441 et ff. (1946).

(11) B. Serin, Phys. Rev. 72, 1261 (1947); A. B. Pippard, G. E. H. Reuter and E. H. Sondheimer, Phys. Rev. 73, 920 (1948).

(12) R. J. Harrison, M.I.T., R.L.E. Quarterly Progress Report p. 29 (Jan. 15, 1948).

(13) M. Desirant and D. Shoenberg, Proc. Phys. Soc. 60, 413 (1940).

(14) E. Laurmann and D. Shoenberg, Nature, 160, 747 (1947).

(15) J. G. Daunt, A. R. Miller, A. B. Pippard and D. Shoenberg, Phys. Rev. 74, 842 (1948).

(16) N. F. Mott and H. Jones, The Theory of the Properties of Metals and Alloys, Oxford (1936).

(17) K. Fuchs, Proc. Camb. Phil. Soc. 34, 100 (1938).